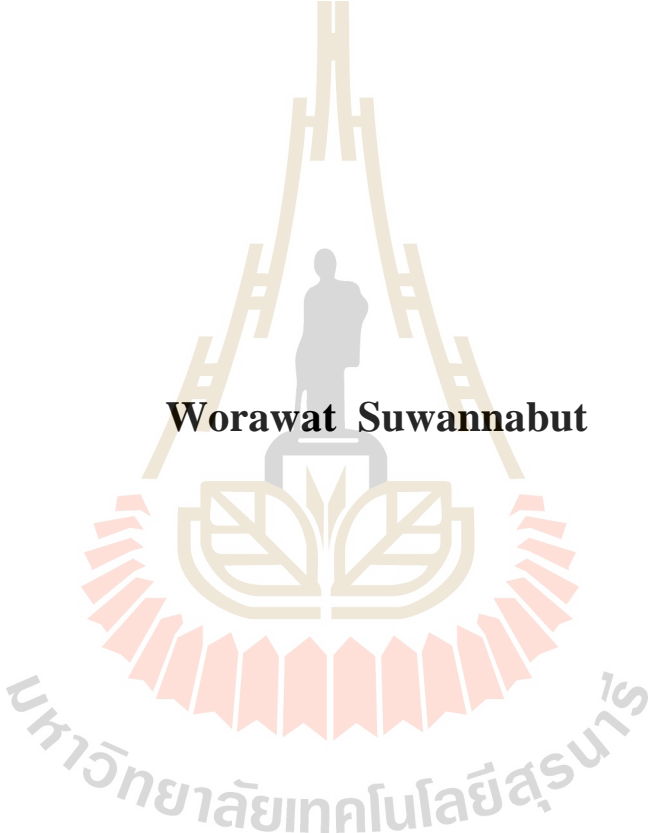


**CONSOLIDATION TEST OF CRUSHED SALT MIXED  
WITH SATURATED MgCl<sub>2</sub> SOLUTION**



**Worawat Suwannabut**

**A Thesis Submitted in Partial Fulfillment of the Requirements for the  
Degree of Master of Engineering in Civil, Transportation and  
Geo-resources Engineering  
Suranaree University of Technology  
Academic Year 2019**

การทดสอบการอัดตัวคายนํ้าของเกร็ดเกลือผสมกับสารละลายแมกนีเซียม  
กลอไรต์อิมตัว



นายวรวัฒน์ สุวรรณบุตร

วิทยานิพนธ์นี้เป็นส่วนหนึ่งของการศึกษาตามหลักสูตรปริญญาวิศวกรรมศาสตรมหาบัณฑิต  
สาขาวิชาวิศวกรรมโยธา ขนส่ง และทรัพยากรธรณี  
มหาวิทยาลัยเทคโนโลยีสุรนารี  
ปีการศึกษา 2561

**CONSOLIDATION TEST OF CRUSHED SALT MIXED WITH  
SATURATED MgCl<sub>2</sub> SOLUTION**

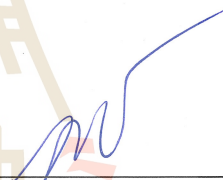
Suranaree University of Technology has approved this thesis submitted in partial fulfillment of the requirements for a Master's Degree.

Thesis Examining Committee



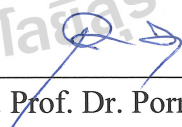
(Asst. Prof. Dr. Akkhapun Wannakomol)

Chairperson



(Asst. Prof. Dr. Decho Phueakphum)

Member (Thesis Advisor)



(Assoc. Prof. Dr. Pornkasem Jongpradist)

Member



(Prof. Dr. Santi Maensiri)

Vice Rector for Academic Affairs  
and Internationalization



(Assoc. Prof. Ft. Lt. Dr. Kontorn Chamniprasart)

Dean of Institute of Engineering

วรวัฒน์ สุวรรณบุตร : การทดสอบการอัดตัวคายน้ำของเกร็ดเกลือผสมกับสารละลาย  
แมกนีเซียมคลอไรด์อิ่มตัว (CONSOLIDATION TEST OF CHUSHED SALT MIXED  
WITH SATURATED  $MgCl_2$  SOLUTION) อาจารย์ที่ปรึกษา : ผู้ช่วยศาสตราจารย์  
ดร. เดโซ เพื่อภุมิ, 71 หน้า.

วัตถุประสงค์ของการศึกษาคือ เพื่อศึกษาคุณสมบัติเชิงกลศาสตร์ของเกลือหินบดผสมกับ  
สารละลายแมกนีเซียมคลอไรด์อิ่มตัวภายใต้ความเค้นและระยะในเวลากการทดสอบการอัดการตัว  
คายน้ำ เกร็ดเกลือผสมกับสารละลายแมกนีเซียมคลอไรด์อิ่มตัวปริมาณ 5 เปอร์เซ็นต์โดยน้ำหนัก  
สำหรับการทดสอบการอัดตัวคายน้ำโดยให้ความเค้นกดคงที่ขนาด 2.5 ถึง 10 เมกะปาสคาล เป็น  
เวลา 7 ถึง 90 วัน ผลการทดสอบระบุว่าความเครียดที่เกิดขึ้นระหว่างการทดสอบอัดตัวคายน้ำมีค่า  
เพิ่มขึ้นอย่างรวดเร็วในช่วง 7 วันแรกและมีแนวโน้มเข้าสู่ค่าคงที่หลังจาก 30 วัน ค่าความหนาแน่น  
กำลังกดสูงสุดในแกนเดียวและสัมประสิทธิ์ความยืดหยุ่นที่ตรวจวัดได้หลังจากการอัดตัวคายน้ำนั้น  
มีค่าเพิ่มขึ้นตามความเค้นและระยะเวลา แต่ในขณะที่ค่าอัตราส่วนปัวซองมีค่าลดลงอย่างช้า ๆ ตาม  
ระยะเวลา กลไกหลักที่ทำให้เกร็ดเกลือหินมีความแข็งและความเหนียวเพิ่มขึ้นคือ การเปลี่ยนแปลง  
ปริมาตรซึ่งเป็นผลอันเนื่องมาจากการจัดเรียงตัวของอนุภาค การแตกและการเชื่อมประสานตัว  
ระหว่างอนุภาคของเกร็ดเกลือ พลังงานความเครียดเฉลี่ยที่เกิดขึ้นจากการอัดตัวคายน้ำของแต่ละ  
ตัวอย่างถูกคำนวณเพื่อใช้ในการคาดคะเนประสิทธิภาพของเกร็ดเกลือสำหรับใช้เป็นวัสดุถมกลับ  
ในช่องเหมือง (คาร์บิลไลต์) ผลการศึกษาพบว่าความลึกและช่วงเวลาที่เริ่มถมกลับของเกร็ดเกลือ  
หลังจากการที่มีการขุดเจาะเป็นปัจจัยสำคัญที่มีผลต่อความหนาแน่น กำลังกด และความยืดหยุ่นของ  
เกลือหินบดในระยะยาว

สาขาวิชา เทคโนโลยีธรณี  
ปีการศึกษา 2561

ลายมือชื่อนักศึกษา วรวัฒน์  
ลายมือชื่ออาจารย์ที่ปรึกษา ดร. เดโซ

WORAWAT SUWANNABUT : CONSOLIDATION TEST OF CRUSHED  
SALT MIXED WITH SATURATED  $MgCl_2$  SOLUTION. THESIS ADVISOR :  
ASST. PROF. DECHO PHUEKPHUM, Ph.D., 71 PP.

BRACKFILL/DENSITY/ELASTIC MODULUS/STRAIN ENERGY

The objective of this study is to determine the mechanical properties of crushed salt mixed with saturated  $MgCl_2$  solution under different stresses and periods of consolidation tests. The crushed salt mixed with 5% by weight of saturated  $MgCl_2$  solution for applied consolidation stresses are 2.5 to 10 MPa for 7 to 90 day. The result indicated that strains during consolidations are increase rapidly within the first 7 days and tend to approach a limit value after 30 days. The density, uniaxial compressive strength and elastic modulus measured after consolidation increase with the stress and duration while the poisson's ratio decreases slowly with time. The mechanisms that strengthen and stiffen the crushed salt mass are consolidation by volumetric change due to particle rearrangement, cracking, and healing between crushed salt particles. The mean strain energy required during consolidation for each specimen is used to predict the crushed salt performance installed in opening excavated in potash (carnallite) mine. Results of the study found that opening depth and installation time after excavation are significant factors governing density, compressive strength and elasticity of the crushed salt backfill in long term.

School of Geotechnology

Academic Year 2018

Student's Signature \_\_\_\_\_ 

Advisor's Signature \_\_\_\_\_ 

## ACKNOWLEDGMENTS

I wish to acknowledge the funding supported by Suranaree University of Technology (SUT).

I would like to express my sincere thanks to Asst. Prof. Dr. Decho Phueakphum for his valuable guidance and efficient supervision. I appreciate his strong support, encouragement, suggestions and comments during the research period. My heartiness thanks to Prof. Dr. Kittitep Fuenkajorn, Dr. Thanittha Thongprapha and Miss Supattra Khamrat for their constructive advice, valuable suggestions and comments on my research works as thesis committee members. Grateful thanks are given to all staffs of Geomechanics Research Unit, Institute of Engineering who supported my work.

Finally, I would like to thank beloved parents for their love, support and encouragement.

Worawat Suwannabut

มหาวิทยาลัยเทคโนโลยีสุรนารี

# TABLE OF CONTENTS

	<b>Page</b>
ABSTRACT (THAI) .....	I
ABSTRACT (ENGLISH).....	II
ACKNOWLEDGEMENTS.....	III
TABLE OF CONTENTS.....	IV
LIST OF TABLES.....	VIII
LIST OF FIGURES .....	IX
SYMBOLS AND ABBREVIATIONS.....	XIV
<b>CHAPTER</b>	
<b>I INTRODUCTION.....</b>	<b>1</b>
1.1 Background and rationale .....	1
1.2 Research objectives.....	2
1.3 Scope and limitations .....	2
1.4 Research methodology.....	3
1.4.1 Literature review .....	3
1.4.2 Sample preparation .....	3
1.4.3 Laboratory testing .....	5
1.4.4 Analysis and assessment .....	5
1.4.5 Applications .....	6
1.4.6 Discussion and conclusion.....	6

## TABLE OF CONTENTS (Continued)

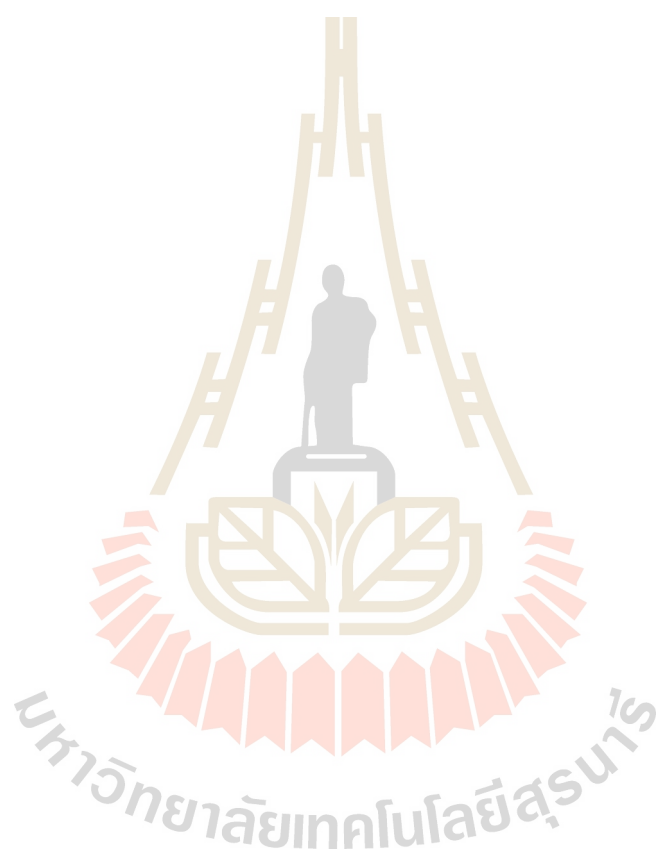
	<b>Page</b>
1.4.7 Thesis writing.....	6
1.5 Thesis contents .....	6
<b>II LITERATURE REVIEW .....</b>	<b>7</b>
2.1 Introduction .....	7
2.2 Effect of brine on rock salt.....	7
2.3 Physical properties of crushed salt consolidation .....	13
2.4 Mechanical properties of consolidated crushed salt .....	14
2.5 Healing mechanisms .....	18
2.6 Effect of particle size .....	20
2.7 Numerical simulation of consolidation crushed salt .....	23
<b>III MATERIAL PREPARATION .....</b>	<b>30</b>
3.1 Introduction.....	30
3.2 Crushed salt sample .....	30
3.3 Saturated MgCl <sub>2</sub> solution.....	30
<b>IV LABORATORY TEST METHOD .....</b>	<b>33</b>
4.1 Introduction.....	33
4.2 Test apparatus .....	33
4.2.1 Test cylinder.....	33
4.2.2 Consolidation load frame.....	33
4.3 Suitable saturated MgCl <sub>2</sub> solution content.....	35

## TABLE OF CONTENTS (Continued)

	<b>Page</b>
4.4 Test method.....	37
4.4.1 Consolidation test.....	37
4.5 Uniaxial compression tests method.....	38
<b>V LABORATORY TEST.....</b>	<b>40</b>
5.1 Introduction.....	40
5.2 Consolidation test results .....	40
5.3 Uniaxial compression test .....	43
<b>VI DERIVATION OF EMPIRICAL EQUATIONS.....</b>	<b>48</b>
6.1 Introduction.....	48
6.2 Strain energy density principle .....	48
6.3. Crushed salt properties as a function of mean strain energy ..	49
<b>VII CRUSHED SALT BLACKFILL PROPERTIES.....</b>	<b>55</b>
7.1 Introduction.....	55
7.2 Long-wall circular opening in salt mass subjected to uniform external pressure .....	55
7.3 Prediction of crushed salt properties after emplacement .....	59
<b>VIII DISCUSSIONS AND CONCLUSIONS.....</b>	<b>64</b>
8.1 Discussions .....	64
8.2 Conclusions.....	69
8.3. Recommendations for future studies .....	70

**TABLE OF CONTENTS (Continued)**

	<b>Page</b>
REFERENCES .....	72
BIOGRAPHY .....	78



## LIST OF TABLES

Table	Page
5.1 Physical properties of crushed salt after consolidation.....	41
5.2 Mechanical properties of crushed salt after consolidation.....	45
6.1 Mean stresses and strains and mean strain energy densities applied to crushed salt during consolidation periods.....	50
7.1 Mechanical and rheological properties of Maha Sarakham salt and carnallite (Wilalak and Fuenkajorn 2016; Luangthip et al. 2016).....	58
8.1 Mechanical properties of crushed salt after consolidation under $\sigma_{\text{cons}} = 10$ MPa for 90 days comparing between crushed salt mixed with NaCl and MgCl <sub>2</sub> (Khamrat et al. 2016).....	68

## LIST OF FIGURES

Figure	Page
1.1 Research methodology.....	4
2.1 Strain-time curves obtained for creep testing of pure halite submerged in halite brine (Theerapun et al., 2017).....	9
2.2 Strain-time curves obtained for creep testing of pure halite submerged in carnallite brine (Theerapun et al., 2017).....	9
2.3 Strain-time curves obtained for creep testing of pure halite submerged in magnesium brine (Theerapun et al., 2017).....	10
2.4 Strain-time curves obtained for creep testing of potash submerged in halite brine (Theerapun et al., 2017).....	10
2.5 Strain-time curves obtained for creep testing of potash submerged in carnallite brine (Theerapun et al., 2017).....	11
2.6 Strain-time curves obtained for creep testing of potash submerged in magnesium brine (Theerapun et al., 2017).....	11
2.7 Weight loss (%) of the carnallite specimens as a function of time under in halite brine (Theerapun et al., 2017).....	12
2.8 Weight loss (%) of the carnallite specimens as a function of time under in carnallite brine (b) (Theerapun et al., 2017).....	12
2.9 Weight loss (%) of the carnallite specimens as a function of time under in magnesium brine (Theerapun et al., 2017).....	13

## LIST OF FIGURES (Continued)

Figure	Page
2.10 Uniaxial compressive strength (a), elastic modulus (b) and Poisson's ratio (c) as a function of consolidation period (t) for different consolidation stresses ( $\sigma_{\text{cons}}$ ) (Khamrat et al., 2016).....	16
2.11 Relationship between inelastic strain in z-direction and densification time for crushed rock salt with water content of 3.17% densified under 15 MPa for 97 days (Miao et al., 1995).....	17
2.12 Compaction as a function of water content and particle size gradation (Ran and Daemen, 1995).....	21
2.13 Evolution of packing density ( $\phi$ ) as a function of the particle aspect ratio ( $\alpha$ ) for different inter-particle friction ( $\mu$ ) (Guises et al., 2009).....	22
2.14 Compressibility percentage of particles shape/size as a function of applied normal stress.....	22
2.15 Numerical predicted and test measured mean strain. (Pudewills and Krauss, 1999).....	25
2.16 Crushed salt fractional density history in a shaft (Callahan and Hansen, 2002).....	25
2.17 Calculated vertical and horizontal closure rates in the test stope (Van Sambeek, 1992).....	28
2.18 Calculated backfill density history for the test stope (Van Sambeek, 1992).....	29

## LIST OF FIGURES (Continued)

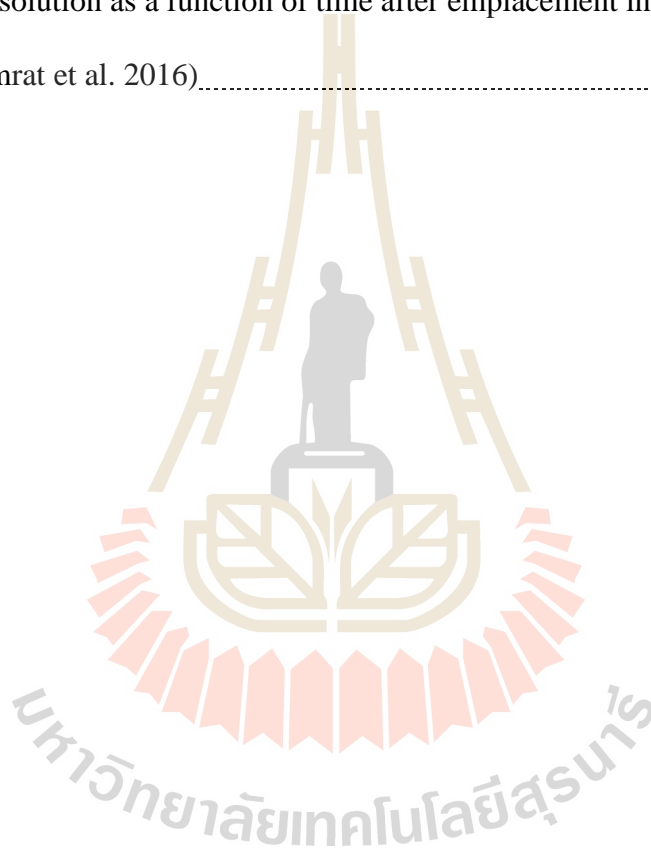
Figure	Page
2.19 Calculated vertical and horizontal backfill stresses in the center of the test stope (Van Sambeek, 1992).....	29
3.1 Crushed salt .....	31
3.2 Sieve analysis apparatus.....	31
3.3 Grain size distribution of crushed salt.....	32
4.1 Cylindrical stainless-steel tube for consolidation testing.....	34
4.2 Laboratory arrangement for consolidation testing.....	34
4.3 Axial strains of consolidation crushed salt with saturated MgCl <sub>2</sub> solution as a function of time for different axial stresses.....	36
4.4 Arrangement for uniaxial compression teste.....	39
5.1 Axial strain (a) and Density (b) as a function of consolidation period (t) for different consolidation stresses ( $\sigma_{\text{cons}}$ ).....	42
5.2 Stress–strain curves obtained from uniaxial compression test of crushed salt specimens after consolidation.....	44
5.3 Density (a), Poisson’s ratio (b), Uniaxial compressive strength (c) and elastic modulus (d) as a function of consolidation period (t) for different consolidation stresses ( $\sigma_{\text{cons}}$ ) of consolidation crush salt mixed with saturated MgCl <sub>2</sub> solution.....	46
5.4 Consolidated specimens before (a) and after (b) uniaxial compression test ...	47
6.1 Density ( $\rho$ ) as a function of mean strain energy density.....	53

## LIST OF FIGURES (Continued)

Figure	Page
6.2 Porosity ( $n$ ) as a function of mean strain energy density.....	53
6.3 Uniaxial compressive strength ( $\sigma_c$ ) as a function of mean strain energy density.....	54
6.4 Elastic modulus ( $E$ ) as a function of mean strain energy density.....	54
7.1 Mean strain energy density ( $W_m$ ) released from closure of circular opening in potash with different carnallite contents ( $C\%$ ) for depths of 200 m and 300 m.....	59
7.2 Remaining mean strain energy density ( $\Delta W_m$ ) as a function of time after backfill emplacement (at year 2) under different carnallite contents ( $C\%$ ).....	61
7.3 Density ( $\rho$ ) of crushed salt backfill as a function of time after emplacement in circular opening for different carnallite contents ( $C\%$ ).....	61
7.4 Porosity ( $n$ ) of crushed salt backfill as a function of time after emplacement in circular opening for different carnallite contents ( $C\%$ ).....	62
7.5 Uniaxial compressive strength ( $\sigma_c$ ) of crushed salt backfill as a function of time after emplacement in circular opening for different carnallite contents ( $C\%$ ).....	62
7.6 Elastic modulus ( $E$ ) of crushed salt backfill as a function of time after emplacement in circular opening for different carnallite contents ( $C\%$ ).....	63

**LIST OF FIGURES (Continued)**

<b>Figure</b>		<b>Page</b>
8.1	Density (a), porosity (b), uniaxial compressive strength (c) and elastic modulus (d) of crushed salt backfill mixed with saturated $MgCl_2$ and $NaCl$ solution as a function of time after emplacement in rock salt (Khamrat et al. 2016).....	66



## SYMBOLS AND ABBREVIATIONS

$\beta$	=	Material constant of the potential creep law
$\Delta\rho_{\text{cons}}$	=	Reduction of bulk density due to the strain energy and consolidation period
$\Delta L$	=	Length change overtime of consolidation crushed salt
$\Delta n_{\text{cons}}$	=	Porosity reduction
$\Delta t$	=	Duration for consolidation
$\Delta W_{\text{m,s}}$	=	Strain energy left for the consolidation is needed
$\epsilon_{\theta}$	=	Tangential strain
$\epsilon_{\text{cons}}$	=	Axial strains of consolidation crushed salt
$\epsilon_{\text{m}}$	=	Mean strain
$\epsilon_{\text{r}}$	=	Radial strain
$\epsilon_{\text{r}}^{\text{c}}$	=	Time-dependent radial strain controlling the creep closure of the opening
$\epsilon_{\text{r}}^{\text{e}}$	=	Elastic radial strain
$\epsilon_{\text{z}}$	=	Axial strain
$\epsilon_1$	=	Major principal strain
$\epsilon_2$	=	Intermediate principal strain
$\epsilon_3$	=	Minor principal strain
$\gamma$	=	Material constants of the potential creep law
$\kappa$	=	Material constants of the potential creep law

## SYMBOLS AND ABBREVIATIONS (Continued)

$\nu$	=	Poisson's ratio
$\rho$	=	Density
$\rho_{\text{cons}}$	=	Density of consolidation crushed salt
$\rho_{\text{H}_2\text{O}}$	=	Density of water
$\rho_{\text{initial}}$	=	Initial density before apply mean strain energy
$\rho_{\text{MgCl}_2.\text{Brine}}$	=	Density of saturated $\text{MgCl}_2$ brine
$\sigma^*$	=	Equivalent (effective) stress
$\sigma_\theta$	=	Tangential stress
$\sigma_r$	=	Radial stress
$\sigma_{\text{cons}}$	=	Consolidation stress
$\sigma_m$	=	Mean stress
$\sigma_r$	=	Radial stress
$\sigma_z$	=	Axial stress
$\sigma_1$	=	Major principal stress
$\sigma_2$	=	Intermediate principal stress
$\sigma_3$	=	Minor principal stress
$a$	=	Opening radius
$C\%$	=	Carnallite content
$E$	=	Elastic modulus
$K$	=	Bulk modulus
$L$	=	Initial Length of installed specimens

## SYMBOLS AND ABBREVIATIONS (Continued)

$L/D$	=	Length-to-diameter ratios
$m$	=	weight of crushed salt specimens
$n$	=	Porosity
$n_{\text{initial}}$	=	Initial crushed salt porosity
$P_o$	=	Uniform external pressure
$r$	=	Radial distance from the opening center
$S.G.MgCl_2.B.$	=	Specific gravity of the saturated $MgCl_2$ brine
$S_r$	=	Radial stress deviation
$T$	=	Time
$t_0$	=	Time at which loading is applied
$t_1$	=	Time at which the strains are calculated
$v$	=	Volume of crushed salt specimens
$W_m$	=	Mean strain energy
$W_{m,l}$	=	Energy lost due to creep closure before backfill is installed
$W_{m,s}$	=	Released strain energy density

# CHAPTER I

## INTRODUCTION

### 1.1 Background and rationale

Potash and salt mines have used the salt tailing as sealing material due to its availability, low cost and physical, chemical and mechanical compatibility with the host rock (Holcomb and Hannum, 1982; Hansen, 1997). The understanding of the consolidation behavior of crushed salt is thus the primary concern for the long-term assessment of the performance of the seal. The factors affecting the mechanical performance of consolidated crushed salt are moisture, duration, consolidation stresses, initial density, particle size and temperature (Shor et al., 1981; Pfeifle et al., 1987). The consolidation is effective only when moisture is available on grain contacts (IT Corporation, 1987; Wang et al., 1992). As a consequence, dry crushed salt shows the lowest consolidation. Case et al. (1987) conclude from their experimental work that the volumetric creep strain rate increases with time and does not reach steady state values even after 1 to 2 months of load application. The uniaxial compressive strength and Young's modulus of crushed rock salt also increase with densification time (Wang et al., 1994; Miao et al., 1995; Somtong et al., 2015; Khamrat et al., 2016). Strengthen and stiffen the crushed salt mass have two main mechanisms simultaneously occur in the crushed salt: (1) consolidation by volumetric change due to particle rearrangement, cracking and creep of the salt crystals, and (2) recrystallization and healing processes (Khamrat et al., 2016). Theerapun et al. (2017) state that carnallite is insensitive to the magnesium brines. The rate of dissolution of specimens in halite brine with higher

carnallite content is higher than those with lower carnallite content. The magnesium brine provides the lowest rate of dissolution. Most researchers have concentrated their effect on the crushed salt mixed with NaCl brine. No attempt has been made to investigate the consolidation behavior of mixtures between crushed salt and MgCl<sub>2</sub> brine. This magnesium brine is often resulted from the potash mine plants, which needs to be disposed safely during the operations.

## **1.2 Research objectives**

The objective of this study is to determine the effectiveness of the crushed salt mixed with saturated magnesium brine (MgCl<sub>2</sub>) for backfilling in potash mine openings. The work involves performing consolidation test on the mixtures. The mechanical properties of consolidated mixture under various durations and applied stresses is determined as a function of the applied mean strain energy densities applied during consolidation. The results is applied as backfill in potash mine openings.

## **1.3 Scope and limitations**

- 1) Crushed salt samples are obtained from the Maha Sarakham formation, Thailand. The grain sizes of crushed salt ranging from 0.075 to 4.75 mm.
- 2) Consolidation tests are performed by applying constant axial stresses to the crushed salt samples installed in 54 mm diameter steel cylinders with length of 200 mm.
- 3) Suitable MgCl<sub>2</sub> brine content is determined.
- 4) Crushed salt specimens are consolidated for 7, 15, 30 and 90 days with applied constant axial stresses of 2.5, 5, 7.5 and 10 MPa.

- 5) Uniaxial compression tests are performed with constant loading rate at 0.1 MPa/s to determine the strength and stiffness of the mixtures.
- 6) All tests are conducted under ambient temperature.
- 7) Up to 16 samples are tested.
- 8) Research findings are published in conference paper or journal.

## **1.4 Research methodology**

The research methodology shown in Figure 1.1 comprises 9 steps; including literature review, sample preparation, consolidation test, uniaxial compression test, physical measurement, analysis and assessment, application, discussions and conclusions, and thesis writing.

### **1.4.1 Literature review**

Literature review is carried out to study researches about salt properties, consolidation testing, physical, mechanical and computer simulations of crushed salt. The sources of information are from journals, technical reports and conference papers. A summary of the literature review is given in the thesis.

### **1.4.2 Sample preparation**

Crushed salt used in this study is prepared from the Lower member salt obtained formation underground openings of ASEAN Potash Mining Co., Ltd. (APMC). They belong to the Lower Salt member of the Maha Sarakham formation, northeastern Thailand. The crushed salts have grain size ranging from 0.075 to 4.75 mm for the consolidation tests. The saturated  $\text{MgCl}_2$  brine is prepared by mixing  $\text{MgCl}_2$  powder with distilled water in plastic tank.

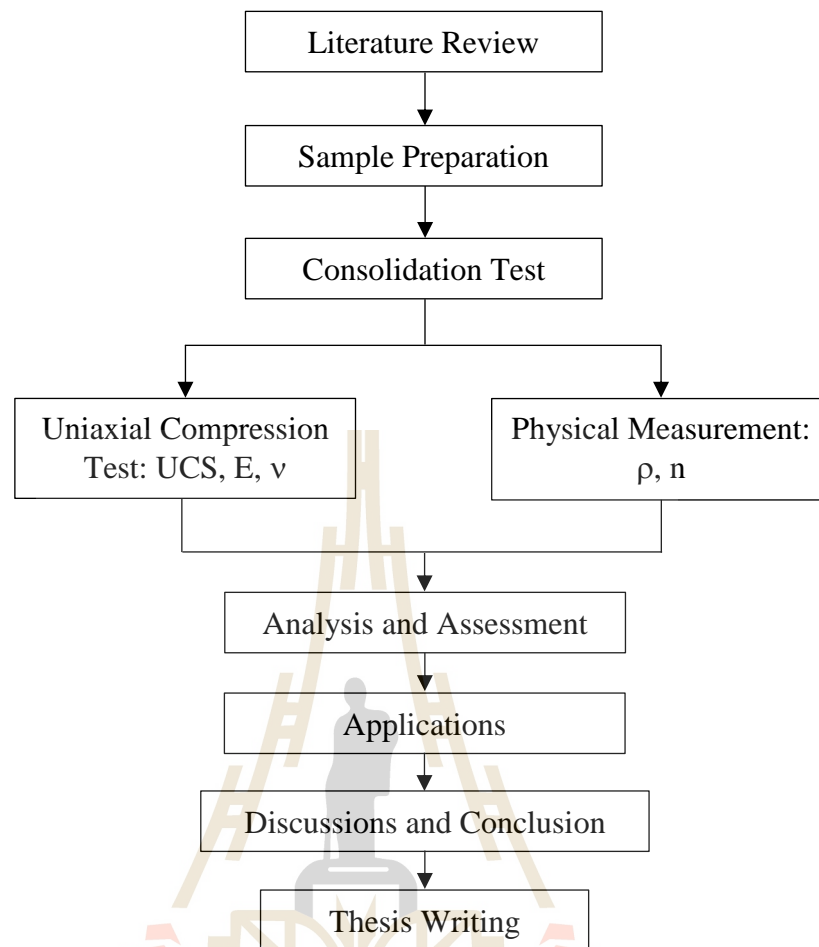


**Figure 1.1** Research methodology.

### 1.4.3 Laboratory testing

The cylindrical steel tube with 54 mm internal diameter, 64 mm outside diameter and 200 mm height is used as consolidation tube. The cylindrical steel tube with 54 mm internal diameter, 64 mm outside diameter and 200 mm height is used as consolidation tube. Two load platens having 53 mm diameter with 100 mm length are to applied axial load to the crushed salt specimens. Two O-rings are installed around each load platen. There is a 10 mm diameter hole at the center of the top and bottom load platens for use as drained hole of water from specimen.

The laboratory testing includes consolidation tests are performed by applying constant axial stresses from a hydraulic load pump to the crushed salt samples installed in the 54 mm diameter steel cylinders. The constant axial stresses are 2.5, 5, 7.5 and 10 MPa. All tests were conducted under ambient temperature. The axial displacements are continuously measured as a function of time by dial gages to calculate the changes of axial strain, density, and void ratio. The compressive strength of the consolidated crushed salts samples is determined by axially loading the crushed salt cylinder (after removing from the steel tube) with a nominal diameter of 54 mm and L/D ranging from 2 to 2.2. Uniaxial compressive strength measurements are made after 7, 15, 30 and 90 days of consolidation.

### 1.4.4 Analysis and assessment

The crushed salt properties are used to develop a set of empirical equations as a function of mean strain energy and consolidation period by SPSS statistical software. The relations are used to predict the crushed salt properties installed in opening under various external pressures and installation periods.

### 1.4.5 Applications

The mean strain energy released by creep closure of openings in infinite salt mass subjected to uniform external pressure (in-situ stress) is determined and used to predict the changes of the crushed salt properties after emplacement.

### 1.4.6 Discussions and conclusions

Discussions of the results are described to determine the reliability and accuracy of the measurements. Performance of the crush salt for sealing material are discussed based on the test results. All research activities, methods, and results are documented and compiled in the thesis. The research or findings are published in the conference proceedings or journals.

### 1.4.7 Thesis writing

All study activities, methods, and results are documented and compiled in the thesis.

## 1.5 Thesis contents

**Chapter I** describes the objectives, the problems and rationale, and the methodology of the research. **Chapter II** presents results of the literature review to improve an understanding of the physical and mechanical properties of consolidated crushed salt mixed with  $MgCl_2$  brine. **Chapter III** describes crushed salt preparation. **Chapter IV** describes the test apparatus and methods. **Chapter V** describes the test result. **Chapter VI** development the empirical equations. **Chapter VII** predict the crushed salt properties after emplacement in mine opening. **Chapter VIII** presents discussions, conclusions and recommendation for future studies.

# CHAPTER II

## LITERATURE REVIEW

### 2.1 Introduction

Relevant topics and previous research results are reviewed to improve an understanding the physical and mechanical properties of consolidation crushed salt mixed with saturated magnesium brine. This review also includes the effect of brine on rock salt, physical and mechanical properties of crushed salt consolidation, healing mechanisms, effect of particle size and numerical simulations. The initial results of literature review are summarized below.

### 2.2 Effect of brine on rock salt

Brodsky and Munson (1991) study the creep on rock salt specimens under saturated NaCl brine introducing around each specimen. Brine around the specimen caused immediately changes in axial, radial, and volumetric strain rates. Strain rates returned to their pre-brine-introduction values for tests conducted with confining pressures more than 3.5 MPa. The results indicate that the effects of moisture do not occur when the confining pressure is sufficiently high to suppress specimen dilation.

Lee and Souza (1998) study the effects of brine contact on the dissolution and strength properties of evaporite ores evaluating operational problems in evaporite deposit utilization associated with brine, halite, sylvinitite, and carnallite ore were creep tested under unconfined conditions, both with and without added brine. Axial deformation and dissolution chemistry were observed throughout the tests. In both

the sylvanite and carnallite ore tests, selective dissolution of sylvite and carnallite minerals was associated with the precipitation of halite. The nature of this process was dependent of temperature and initial brine and ore composition. Generally, the presence of brine caused a decrease in the resistance to creep deformation and increase more mechanism fracture. It is suggested that observed weakening in evaporites under dilatant conditions and in the presence of brine is due primarily to the enhancement of fracture mechanics processes through selective dissolution from stressed areas in the rock, such as fracture-process zones and asperities acting as barriers to slip.

Theerapun et al. (2017) study the effects of various backfill compositions on the integrity of rooms and pillars in salt and potash mines. Uniaxial creep tests are performed on halite and carnallite core specimens for up to 21 days. The constant axial stresses are varied from 2 to 12 MPa. After the specimens are under loading for 7 days, they are separately submerged in three types of solutions prepared from halite, carnallite and magnesium chloride. The solution is removed after 7 days. The results indicate that the specimens that are composed of pure halite is insensitive to these solutions, as evidenced by that the creep strain rates measured before, during and after brine submersion remain unchanged (Figure 2.1, 2.2 and 2.3). The specimens containing carnallite of 30% to 90% by weight are sensitive to halite and carnallite solutions, but insensitive to magnesium chloride solution (Figure 2.4, 2.5 and 2.6). The percentage weight loss of the carnallite specimens during submersion in these solutions confirm that saturated magnesium brine has insignificant effect on the dissolution of the carnallite specimens (Figure 2.7, 2.8 and 2.9). The findings can be used for the material selection and the performance assessment of the installed backfill compositions in salt and potash mines.

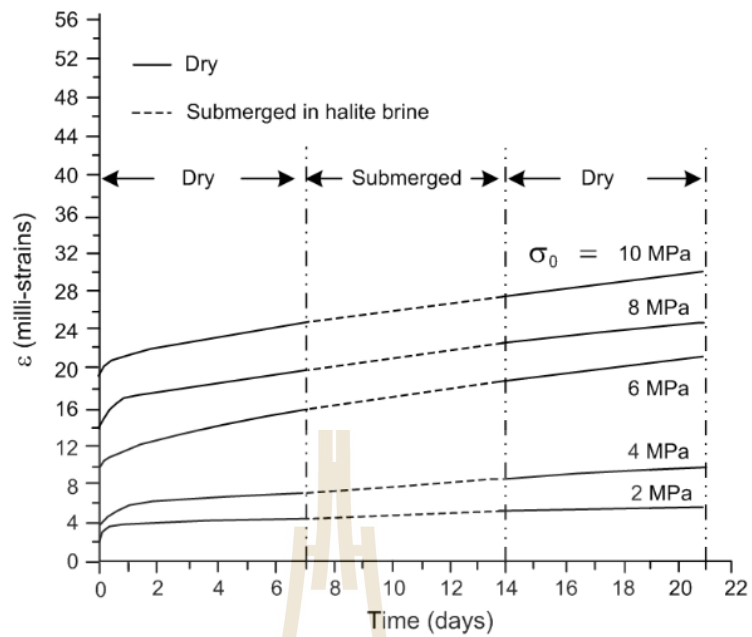


**Figure 2.1** Strain-time curves obtained for creep testing of pure halite submerged in halite brine (Theerapun et al., 2017).

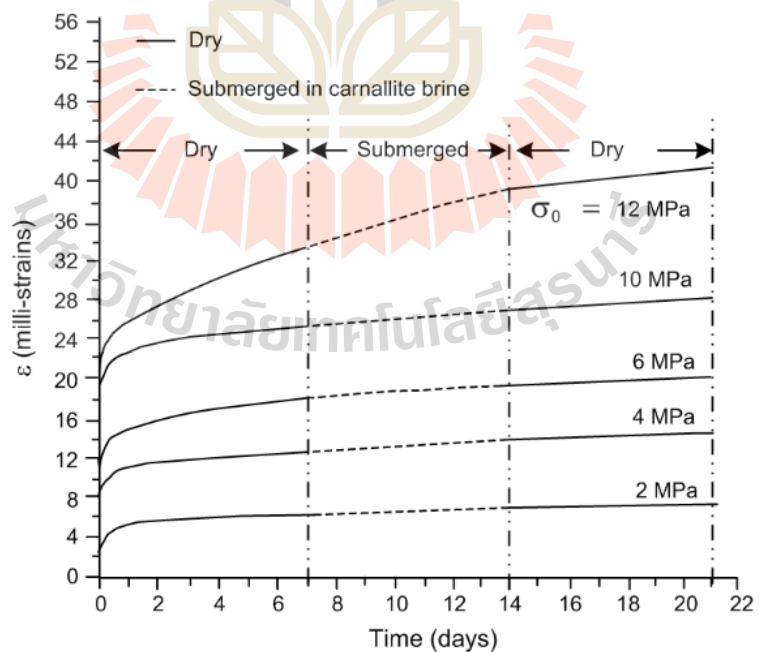


**Figure 2.2** Strain-time curves obtained for creep testing of pure halite submerged in carnallite brine (Theerapun et al., 2017).

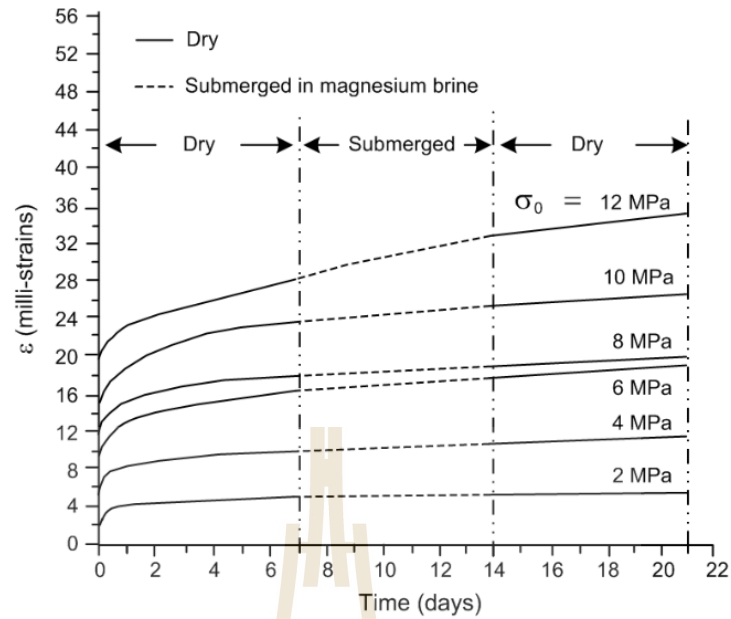


**Figure 2.3** Strain-time curves obtained for creep testing of pure halite submerged in magnesium brine (Theerapun et al., 2017).

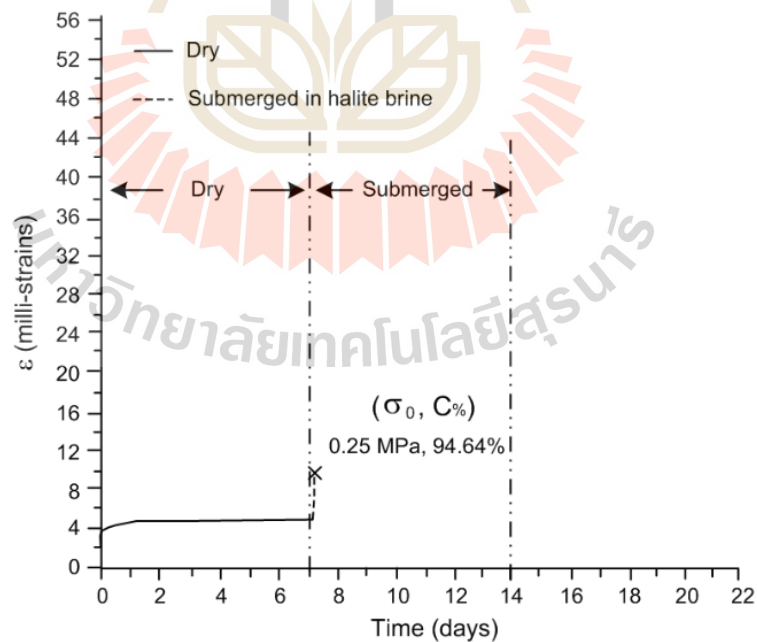


**Figure 2.4** Strain-time curves obtained for creep testing of potash submerged in halite brine (Theerapun et al., 2017).

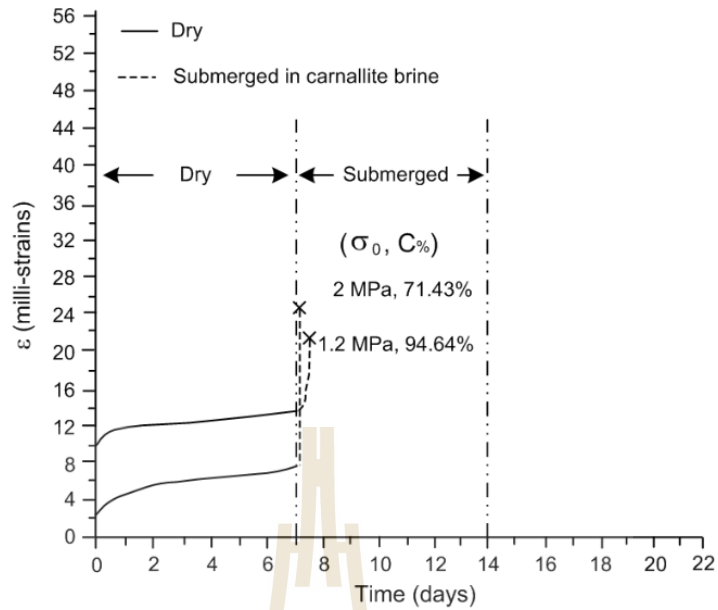


**Figure 2.5** Strain-time curves obtained for creep testing of potash submerged in carnallite brine (Theerapun et al., 2017).

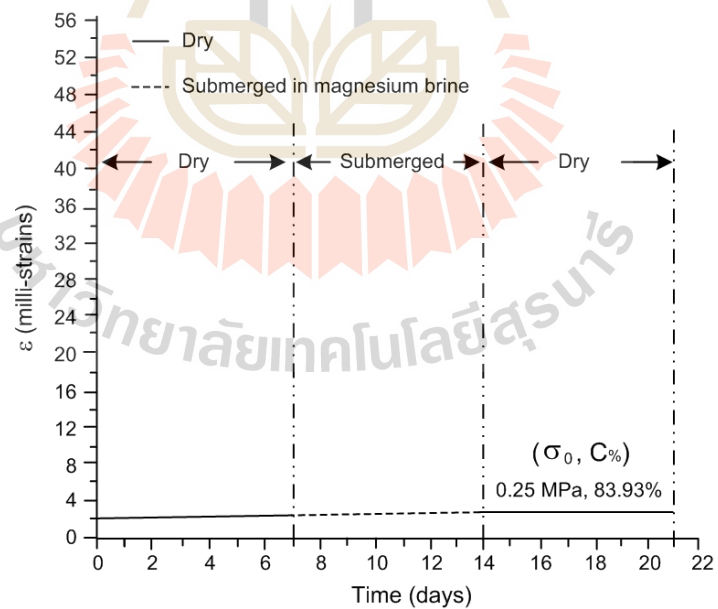


**Figure 2.6** Strain-time curves obtained for creep testing of potash submerged in magnesium brine (Theerapun et al., 2017).

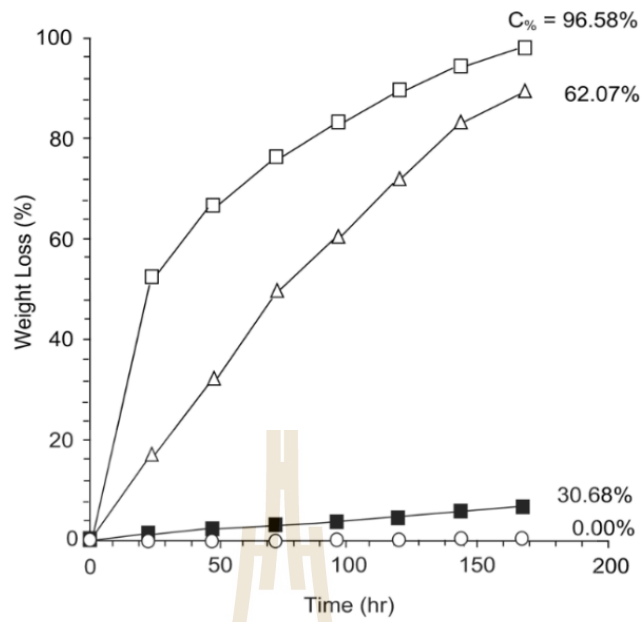


**Figure 2.7** Weight loss (%) of the carnallite specimens as a function of time under in halite brine (Theerapun et al., 2017).

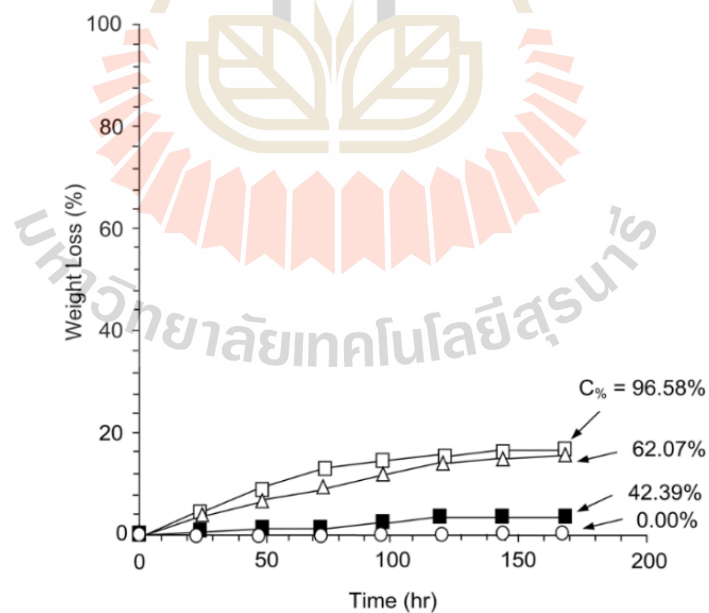


**Figure 2.8** Weight loss (%) of the carnallite specimens as a function of time under in carnallite brine (b) (Theerapun et al., 2017).

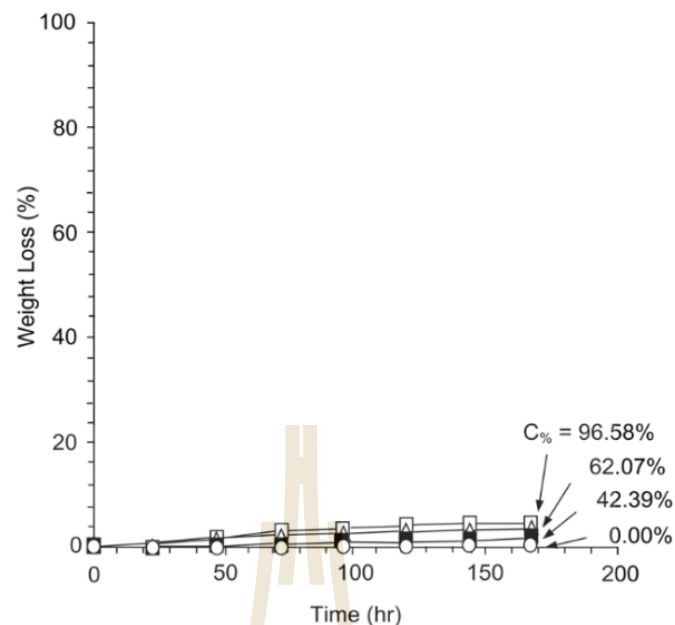


**Figure 2.9** Weight loss (%) of the carnallite specimens as a function of time under in magnesium brine (Theerapun et al., 2017).

### 2.3 Physical properties of crushed salt consolidation

The compaction of crushed salt increase with increasing water content until the optimum water content is reached, that equal to 5% brine by weight (Ran and Daemen, 1995). Consolidation of crushed salt increases with increasing brine content until the optimum brine content is reached, which is 5% by weight. The volumetric strain and density increase with consolidation stresses and time. The highest density observed for 10 MPa consolidation stress for 15 days which equal to  $2.04 \text{ g/cm}^3$  and predictions density of consolidated crushed salt will be similar intact salt ( $2.2 \text{ g/cm}^3$ ) after 12 months under mean stress equal 4 MPa (Somtong et al., 2015).

Wang et al. (1992) conduct several series of densification tests on crushed rock salt with water contents varying from 0.12% to 4.72%. The compaction of crushed salt increase with increasing brine content until the optimum brine content is reached and

decreases with further brine content increases. The unconfined compressive strength and Young's modulus of crushed rock salt also increase with respect to densification time and decreases with porosity (Kelsall et al., 1984). The relationship between void ratio and time is found to be exponential equations (Olivella and Gens, 2002). The initial porosity and permeability decrease with increasing density (Case and Kelsall, 1987; Loken and Statham, 1997; Hansen and Mellegard, 2002; Salzer et al., 2007). Brodsky et al. (1995) conducted hydrostatic and triaxial compression tests with brine content of 2.5% to 3% by weight. The results indicate that the permeability decreases approximately orders of magnitude as fractional density increases from 0.9 to 1.

#### **2.4 Mechanical properties of consolidated crushed salt**

Kelsall et al. (1984) explain the properties of crushed salt and the nature of fracture healing as known from laboratory testing and presents analytical methods for predicting the rates at which the processes will occur in a repository. The range of grain size for the crushed material is 75 mm to about 0.05 mm. The results indicate that consolidations to low porosities should occur within hundreds of years at most candidate repository sites for locations within the repository close to the waste.

Pfeifle et al. (1987) perform the hydrostatic compression creep tests of crushed salt specimen from Avery Island dome salt. The experiments are performed to assess the influence of the following four variables on the consolidation and unconfined strength of crushed salt: grain size distribution, temperature, time, and moisture content. The levels of each variable investigated are grain size distribution, uniform-graded and well-graded (coefficient of uniformity of 1 and 8); temperature 25 °C and 100 °C; time,  $3.5 \times 10^3$  s and  $950 \times 10^3$  s (approximately 60 minutes and 11 days, respectively) and

moisture content, dry and wet (85 percents relative humidity for 24 hours). The hydrostatic creep stress is 10 MPa. The unconfined compression tests are performed at an axial strain rate of  $1 \times 10^{-5} \text{ s}^{-1}$ . Results show that the variables time and moisture content have the greatest influence on creep consolidation, while grain size distribution and, to a somewhat lesser degree, temperature have the greatest influence on total consolidation. Time and moisture content and the confounded two-factor interactions between either grain size distribution and time or temperature and moisture content have the greatest influence on unconfined strength.

Somtong et al. (2015) determine the strength and deformability of crushed salt as affected by applied stresses and consolidation period. The crushed salt has grain sizes ranging from 0.075 to 4.76 mm. The optimum brine content is determined as 5% by weight. The consolidation tests are performed by applying constant axial stresses to the crushed salt samples installed in the 54 mm diameter steel cylinders. The axial stresses are 2.5, 5, 7.5 and 10 MPa. The results indicate the uniaxial compressive strength and elastic modulus increase with the consolidation magnitude and period. The lowest compressive strength is observed for 2.5 MPa consolidation stress at 3 days. The highest compressive strength is observed for 10 MPa consolidation stresses which is about 8.1 MPa. The elastic modulus is 4.10 GPa after 15 days of consolidation.

Khamrat et al. (2016) perform consolidation tests to determine the mechanical properties of crushed salt as affected by applied stresses and consolidation period. The crushed salt with particle sizes ranging from 0.075 to 4.76 mm mixed with 5% saturated brine are consolidated under axial stresses ranging from 2.5 to 10 MPa. The densities, uniaxial compressive strengths and elastic moduli measured after consolidation for 3–180 days increase with applied stresses and time (Figure 2.10).

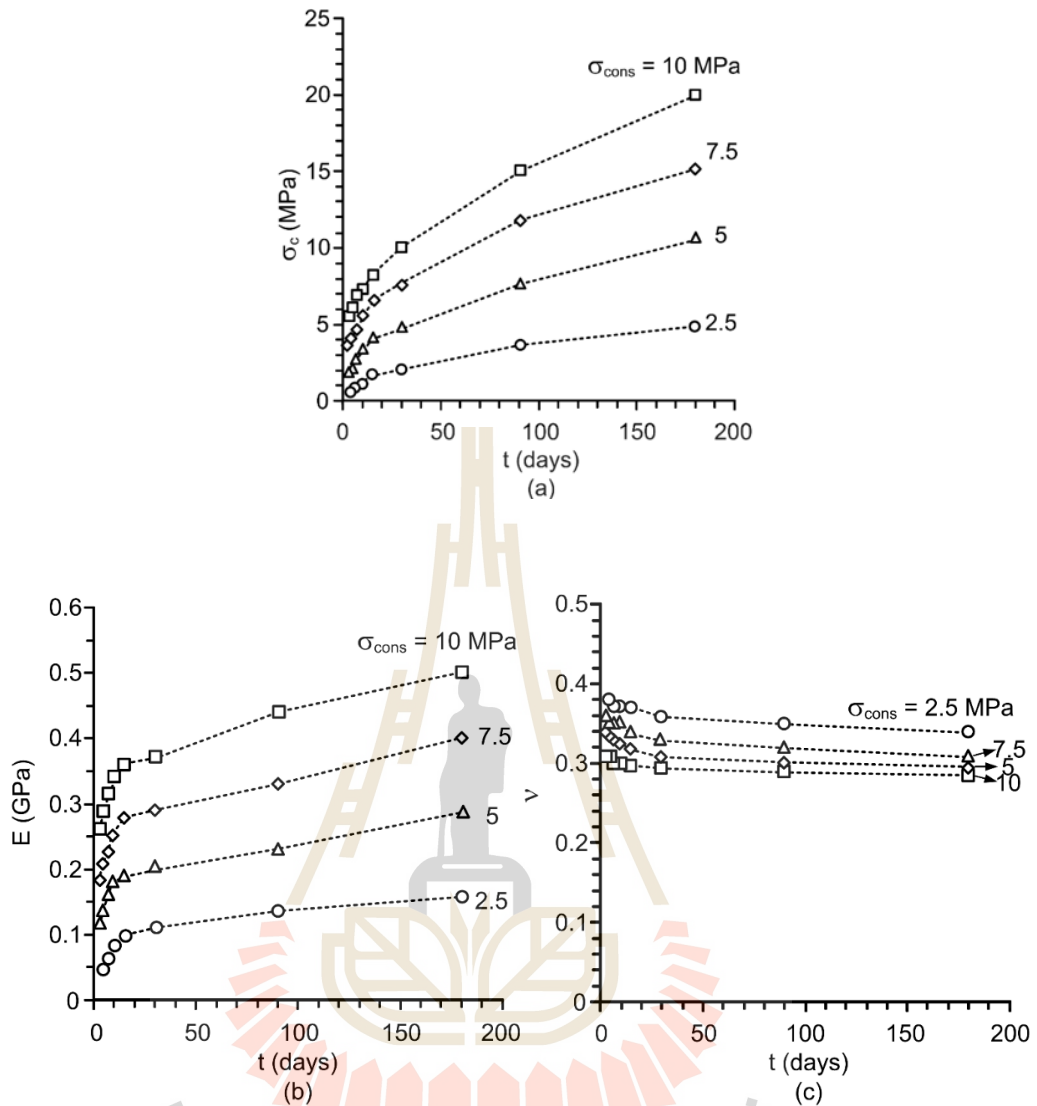


**Figure 2.10** Uniaxial compressive strength (a), elastic modulus (b) and Poisson's ratio (c) as a function of consolidation period ( $t$ ) for different consolidation stresses ( $\sigma_{\text{cons}}$ ) (Khamrat et al., 2016).

Miao et al. (1995) propose constitutive models for healing of materials with application to compaction of crushed rock salt. The crushed rock salt samples were sieved and remixed into a gradation with maximum particle sizes of 4.76 mm, the optimum water content for crushed rock salt densified are equal to 3.0% by weight. The result indicate that the increase of Young's modulus is one of the main features of healing processes in which void space is reduced and the bonding force between particles is enhanced because of the diffusion and recrystallization that occur on the grain boundaries. Besides Young's modulus, strength, and vertical inelastic strain of densified crushed rock salt also increase with respect to densification time, as shown in Figure 2.11.

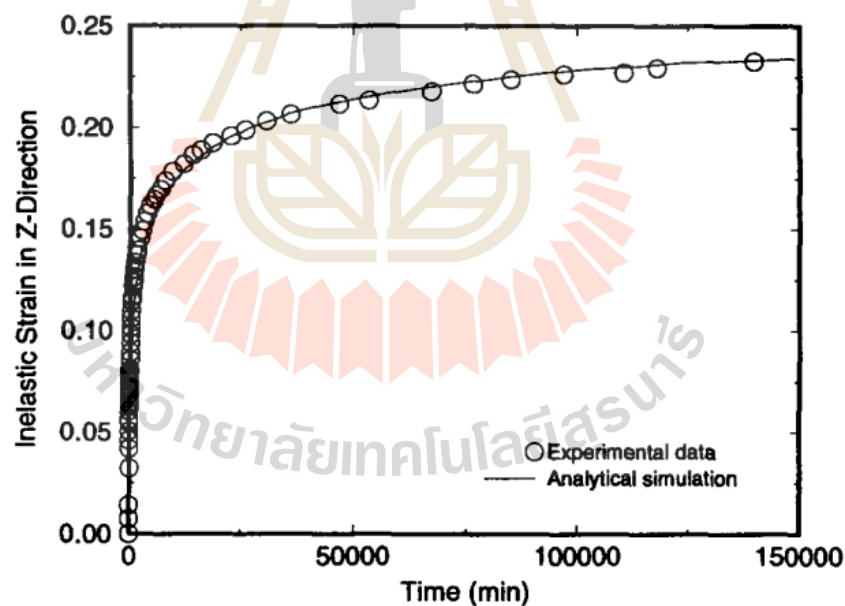


**Figure 2.11** Relationship between inelastic strain in z-direction and densification time for crushed rock salt with water content of 3.17% densified under 15 MPa for 97 Days (Miao et al., 1995).

Pfeifle (1991) determines consolidation, permeability, and compressive strength of specimen prepared from bentonite/crushed salt mixtures. Each mixture comprised 30 percent bentonite and 70 percent crushed salt based on total dry weight. Brine was added to each mixture to adjust its water content to either 5 or 10 percent by weight. The consolidation tests are conducted under hydrostatic stresses between 3.45 and 14 MPa. The volumetric strains increase between 0.2 and 0.3 with increasing hydrostatic stress and consolidation time. Constant rate of flow test show that permeability ranging from  $1.3 \times 10^{-17}$  m<sup>2</sup> to  $4.9 \times 10^{-17}$  m. The unconfined compressive strength is ranging from 0.5 to 8.1 MPa. The higher strengths are measured at higher densities.

## 2.5 Healing mechanisms

Hwang et al. (1993) conducted the environmental scanning electron microscope (ESEM) to study the grain boundary healing behavior of crushed rock salt and the consolidation mechanism of rock salt backfill. The specimens were then put on the cold stage inside the ESEM chamber. Consolidation specimens with water content varying from 0.54-4.72 % by weight were uniaxially consolidated under a low pressure of 3 MPa at a temperature of 25 °C. The specimens were prepared by taking 3.0 mm cores from solid rock salt and then split to a slice of 0.1 mm thickness. The result indicate that the consolidation of crushed rock salt is governed by contact translation, with or without rotation mechanisms at a suitable moisture content, crushing and shearing at the lower moisture content, and sliding at the higher moisture content. Direct observation of specimens in the ESEM resulted in viewing water trapped on the surface and the formation of a water meniscus between two particles. The concentration of

brine at the grain boundary was observed as contributing to the amount of recrystallization. The amount of water therefore has a great effect on the consolidation of rock salt and is possibly due to the sliding, rotation, or crushing of the contact zone of the granular material.

Miao et al. (1995) state that the healing mechanics is a suitable theory for describing the mechanical behavior of healing materials. With simplifying assumptions, healing evolution equations based on a scalar isotropic evolution equation for change in elasticity are given. The comparison between a limited amount of experimental data and model simulation on densification of crushed rock salt under uniaxial strain loading conditions.

Khamrat et al. (2016) state that the main mechanisms govern the changes of the properties of crushed salt are consolidation and recrystallization. The first mechanism involves the volumetric reduction of the crushed salt mass by particle rearrangement, creep, cracking and sliding between grain boundaries. The second mechanism involves the recrystallization and healing between salt particles.

Down and McMullen (1985) use scanning electron microscopic techniques (SEM) to observe the epoxy pore structure replica of sodium chloride compact storage for controlled humidity from 12 - 94% RH. A result of extensive recrystallization occurring between particle faces. Recrystallization is demonstrated to be a response to local crystal lattice dislocations caused by interparticulate friction during compaction. The recrystallization increases with increasing time at all humidities.

IT Corporation (1987) investigates the consolidation behavior of crushed salt and fracture healing in natural and artificial salt. The fracture healing program included permeability tests conducted on fractured and unfractured samples. The tests are

conducted in a Hoek cell at hydrostatic pressures up to 3,000 psi (20.6 MPa) with durations up to 8 days. For the natural rock salt tested, permeability is strongly dependent on confining pressure and time. The effect of confining pressure is much weaker in the artificial salt. In most cases the combined effects of time and pressure are to reduce the permeability of fractured samples to the same order of magnitude (or less) as the permeability measured prior to fracturing.

## 2.6 Effect of particle size

Wang et al. (1994) study the densification processed of crushed salt consolidation. The sample has been remixed into three gradation types with maximum particle sizes of 4.76, 2.36 and 1.18 mm. The results show the increase of consolidation rate of consolidated crushed salt when average particle size decreases.

Ran and Daemen (1995) study and present results of laboratory compaction testing to determine the influence of particle size, size gradation and moisture content on compaction of crushed rock salt. The compaction increases with maximum particle size and compaction energy and varies significantly with particle size gradation and water content until the optimum water content is reached (5%) and decreases with further water content increases (Figure 2.12).

Guises et al. (2009) present an application of a recently improved numerical simulation technique for deformable granular material with arbitrary shapes for study on the influence of the effect of the particle shape on the emergent properties of a granular pack (packing density, coordination number, force distribution). The result indicate that the packing density are increased with the particle ellipse aspect ratio  $\alpha$

and the packs built with an aspect ratio lower than  $\alpha = 1.6$  possess a reasonably constant. The contact friction can be decreased the packing density (Figure 2.13).

Fu et al. (2012) presents the influence of particles shape/size of three different lactose powders on dynamic characteristics by compressibility test. Two of the samples differ in size but have similar shapes; the third sample is more spherical but similar in size to one of the other two samples. The result indicates that the compressibility percentage of particles shape/size are increase with increasing normal stress (Figure 2.14).

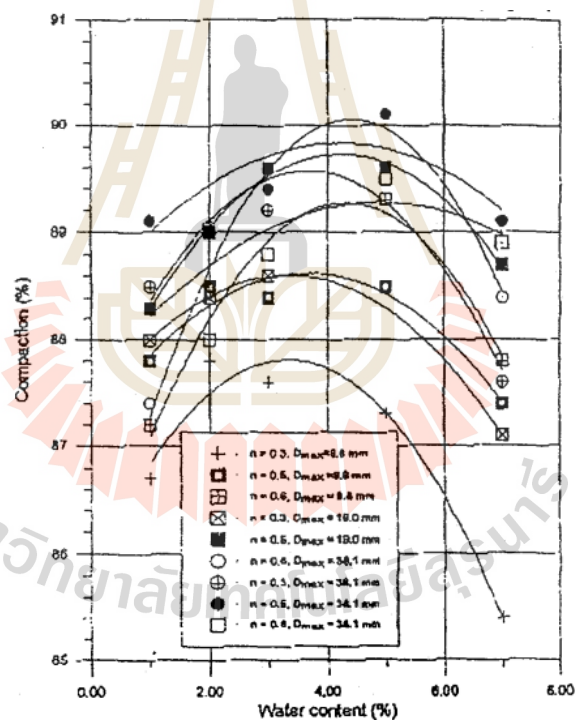


**Figure 2.12** Compaction as a function of water content and particle size gradation (Ran and Daemen, 1995).

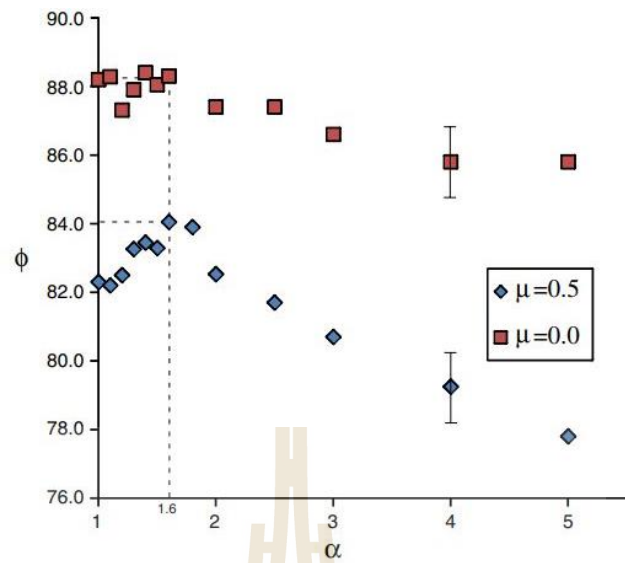


**Figure 2.13** Evolution of packing density ( $\phi$ ) as a function of the particle aspect ratio ( $\alpha$ ) for different inter-particle friction ( $\mu$ ) (Guises et al., 2009).

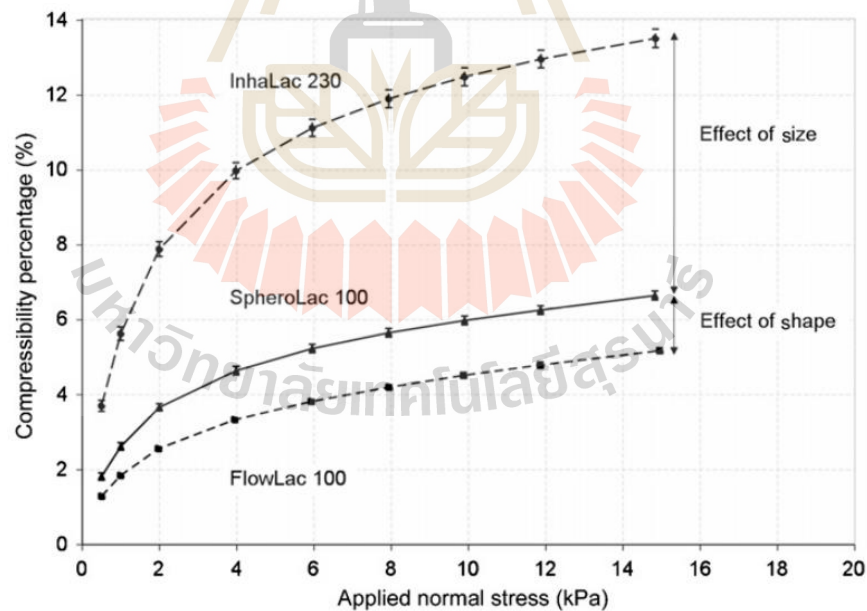


**Figure 2.14** Compressibility percentage of particles shape/size as a function of Applied normal stress.

## 2.7 Numerical simulations of consolidation crushed salt

Pudewills and Krauss (1999) present the numerical modeling of the thermomechanical behavior of crushed salt using a viscoplastic constitutive model. In the ADINA finite element code the viscoplastic model that considers both volumetric and deviatoric strain rates under hydrostatic and shear stress conditions proposed by Hein (1991) is implemented. A series of exercises were designed to verify the numerical implementation and the theoretical formulation of the proposed model. The applicability of the model to predicting the consolidation of a crushed salt specimen with step-wise stress increase and decrease, performed in laboratory tests. Mathematical equation proposed by Hein (1991) is as follows:

$$\dot{\varepsilon}_{ij} = A \cdot \exp^{-Q/RT} \cdot (h_1 \cdot p^2 + h_1 \cdot q^2)^n \cdot \left( \frac{1}{3} h_1 \cdot p \cdot I + h_2 S_{ij} \right) \quad (2.1)$$

$$h_1 = \frac{a}{\left[ \left( \left( \frac{\eta_0}{\eta} \right)^c - 1 \right) / \eta_0^c + d \right]^m} \quad (2.2)$$

$$h_2(\eta) = b \cdot h_1(\eta) + 1 \quad (2.3)$$

where  $\varepsilon_{ij}$  is the strain occurring,  $\eta$  is the porosity,  $\eta_0$  is the initial porosity,  $T$  is the absolute temperature,  $p$  is the mean stress perpendicular,  $I$  was the Tensor metric,  $Q$  is the activation energy,  $R$  is the gas constant,  $q$  is the a variation of stress  $S_{ij}$  is the stress deviation tensor,  $A$ ,  $b$ ,  $c$ ,  $d$ ,  $m$ ,  $n$  are constants of the equation, and the  $Q/R$  is a constant equal to  $6520 \text{ K}^{-1}$  of the consolidation (Odometer test) with strain rate  $6.9 \times 10^{-9} \text{ s}^{-1}$ . The results are consistent with the results of laboratory tests. The simulation model and compression stresses increase to 3 levels by 15 days/step, compared to the average

stress and the changes of porosity. The results of simulation and experiment were found to be consistent as well. The simulation results will provide a slightly lower value (Figure 2.15).

Callahan and Hansen (2002) use the finite element program SPECTROM-32 to predict the creep deformation of the host rock and the consolidation of the crushed salt seal material in the shafts. The shaft is assumed to be open for 50 years and then instantaneously filled with crushed salt dynamically compacted to a fractional density of 90 percent. Crushed salt is emplaced within the shafts at depths ranging from 430 meters to 600 meters. Figure 2.16 presents the results of six shaft seal analyses using the shear and combined database parameter value sets at three different depths. At depths of 600 m, 515 m and 430 m approximately 60 years, 110 years and 240 years, respectively, are required to attain a crushed salt fractional density of 99 percent. These results show that the responses for either parameter value set at each depth are similar up to a fractional density of about 98 percent. Therefore, the model results diverge slightly consolidation. The results also indicated that the shear parameter values set predicts the fastest rate.

Callahan et al. (1996) develop the constitutive models to describe the deformation of crushed salt. The candidate constitutive models are generalized to three-dimensional states of stress to include the effects of mean and deviatoric stress and modified to include the effects of temperature, grain size, and moisture content. A database including hydrostatic consolidation and shear consolidation tests conducted

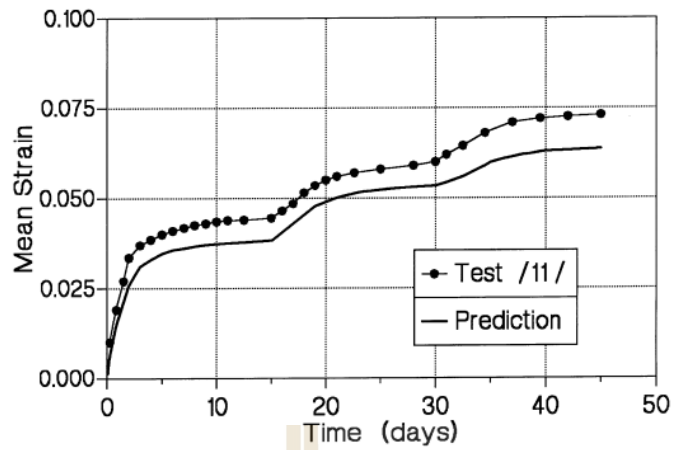


**Figure 2.15** Numerical predicted and test measured mean strain. (Pudewills and Krauss, 1999).

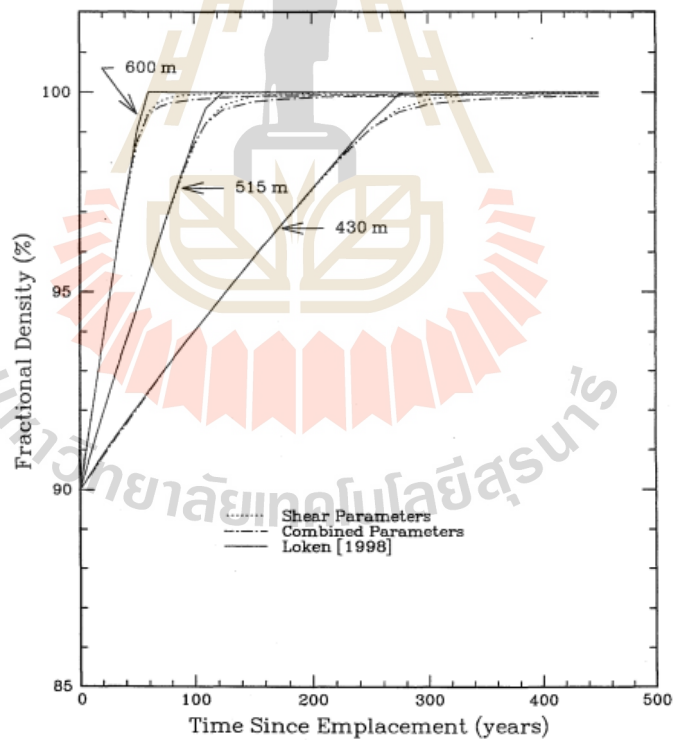


**Figure 2.16** Crushed salt fractional density history in a shaft (Callahan and Hansen, 2002).

on Waste Isolation Pilot Plant (WIPP) and southeastern New Mexico salt is used to determine material parameters for the candidate constitutive models. The total strain rate for the crushed-salt constitutive model is assumed to consist of three components. The components include nonlinear elastic ( $\varepsilon_{ij}^e$ ), consolidation ( $\varepsilon_{ij}^c$ ), and creep ( $\varepsilon_{ij}^i$ ) contributions, and the total strain rate is written as the sum of these rates:

$$\varepsilon_{ij} = \varepsilon_{ij}^e + \varepsilon_{ij}^c + \varepsilon_{ij}^i \quad (2.4)$$

Both the nonlinear elastic and consolidation portions of the model describe the material behavior in bulk (volumetric) and in shear (deviatoric). Following the approach of Fossum et al. (1988), the three-dimensional generalization of the kinetic equation for the consolidation inelastic flow is:

$$\varepsilon_{ij}^c = \varepsilon_{eq}^c(\sigma_{eq}^f) \left( \frac{\partial \sigma_{eq}}{\partial \sigma_{ij}} \right) \quad (2.5)$$

where  $\varepsilon_{ij}^c$  is the inelastic strain rate tensor and  $\sigma_{eq}^f$  and  $\varepsilon_{eq}^c$  are the power-conjugate equivalent stress measure and equivalent inelastic strain rate measure for creep consolidation, respectively. The effects of moisture, particle size and temperature are combined to form parameter ( $\xi$ ), which is incorporated as a multiplicative constant on the equivalent inelastic strain rate:

$$\xi = (L/d_p) [1 + a_1 (\exp(a_2 w))] \exp(-Q_c/RT) \quad (2.6)$$

where:  $w$  = moisture fraction by weight,  $a_1$ ,  $a_2$  = material parameters,  $d$  = average grain diameter [m],  $p$  = material parameter,  $L$  = dimensional parameter [ $m^p$ ],  $R$  = universal gas constant [J/(mol-K)],  $T$  = absolute temperature [K] and  $Q_c$  = material parameter [J/mol].

Three models were selected for evaluation; i.e, those attributed to Sjaardema Krieg, Zeuch, and Spiers. The models were generalized to three-dimensional forms and modified where deemed necessary. A database comprised of hydrostatic and shear consolidation tests was created and used to determine the material parameters of the candidate constitutive models. Rank ordering of the statistical measures obtained from the model fitting indicates that the modified Spiers model is moderately superior to the other two models. The new stress dependence and generalization enable the models to represent crushed salt behavior under deviatoric stresses.

Van Sambeek (1992) presents the technology developed for calculating the behavior of crushed salt backfill at the Waste Isolation Pilot Plant (WIPP) near Carlsbad, New Mexico. This technology includes laboratory testing results, material constitutive laws, modeling results, and field measurements. Two types of laboratory tests are common: isostatic and odometer consolidation. The consolidation model adopted by the WIPP program for granular halite comprises a total strain rate consisting of three components: nonlinear elastic, creep, and thermal strain. The consolidation data are used to determine the constant parameters in the consolidation model for used in the numerical model. The numerical modeling is used to simulate the crushed salt backfill in potash mine opening with 42 m wide, 4 m room high and 63 m pillars wide under stress field of 20 MPa. The results show that before the backfill is placed, the closure rates had become nearly constant (a steady-state closure rate) (Figure 2.17).

Even after the backfill is placed, the constant closure rate is sustained until 3.6 years (2.2 years after backfill placement). By that time, consolidation of the backfill had caused the density to increase to slightly more than 1,600 kg/m<sup>3</sup> (Figure 2.18) and a 0.5 MPa pressure had developed in the backfill (Figure 2.19). Beyond 3.6 years, the backfill pressure increased (and room closure rate decreased) steadily as additional consolidation occurred. The complete consolidation is achieved by about 10 years and the backfill pressure had reached about 10 MPa.

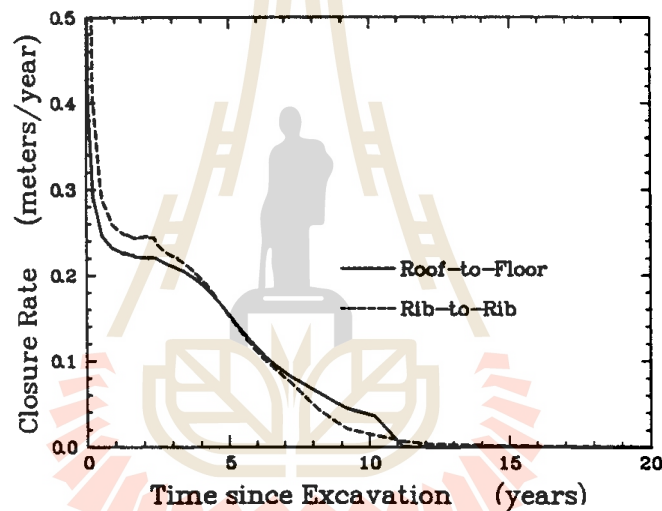


**Figure 2.17** Calculated vertical and horizontal closure rates in the test stope (Van Sambeek, 1992).

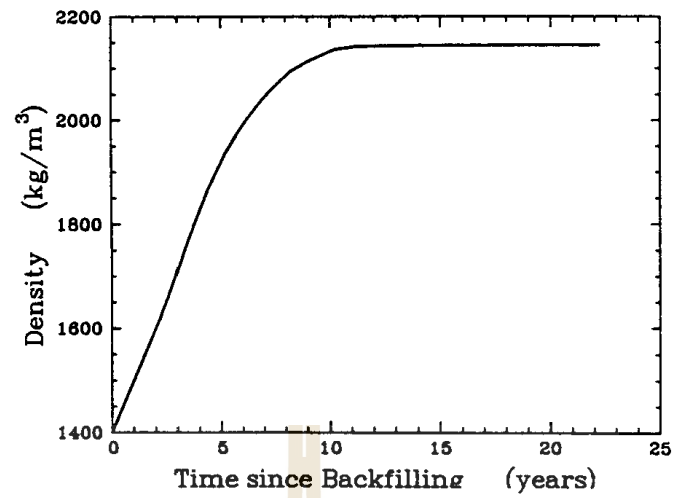


**Figure 2.18** Calculated backfill density history for the test stope (Van Sambeek, 1992).

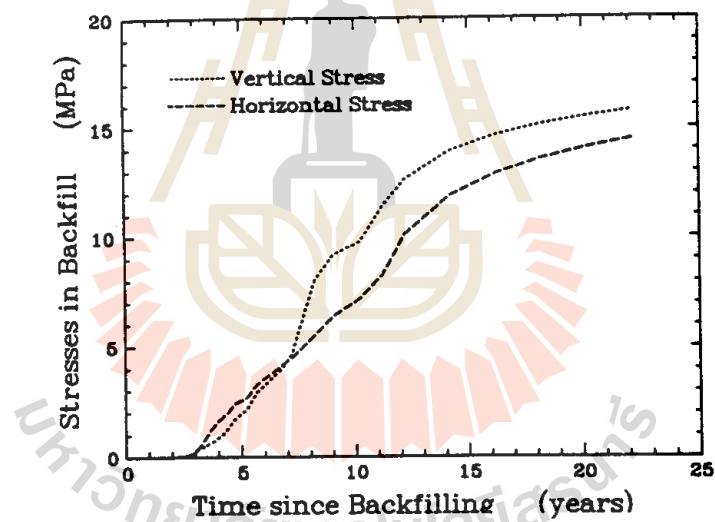


**Figure 2.19** Calculated vertical and horizontal backfill stresses in the center of the test stope (Van Sambeek, 1992).

## **CHAPTER II**

### **LITERATURE REVIEW**

#### **3.1 Introduction**

This chapter describes the crushed salt and saturated  $\text{MgCl}_2$  solution preparation to be used in the consolidation test. The crushed salt is obtained from the Lower member of the Maha Sarakham formation in the Korat basin, northeastern Thailand.

#### **3.2 Crushed salt sample**

The crushed salt sample in this study has been prepared from Lower member of Maha Sarakham formation. The salt blocks were donated by ASEAM Potash Chaiyaphum Co., Ltd. (APOT). They are crushed by hammer mill (2HP-4 POLES, Spec jis c-4004). The grain size of crushed salt ranges from 0.075 to 4.75 mm (Figure 3.1). The grain size distribution can be determined by sieve analysis (Figure 3.2). The crushed salt is passing through sieve numbers 4, 10, 20, 40, 60, 100 and 200 (Figure 3.3). This size range is equivalent to those expected to be obtained as waste product from the mines.

#### **3.3 Saturated $\text{MgCl}_2$ solution**

Saturated  $\text{MgCl}_2$  solution is prepared by mixing  $\text{MgCl}_2$  tablets with distilled water. The  $\text{MgCl}_2$  tablets is added until no dissolution does not occurs. The proportion of  $\text{MgCl}_2$  tablets to water under saturation is 57% by weight. Specific gravity of the saturated  $\text{MgCl}_2$  solution ( $\text{S.G.}_{\text{MgCl}_2, \text{B}}$ ) is calculated as  $\text{S.G.}_{\text{MgCl}_2, \text{B}} = \rho_{\text{MgCl}_2, \text{B}} / \rho_{\text{H}_2\text{O}}$ ,

where  $\rho_{\text{MgCl}_2, \text{B}}$  is density of saturated  $\text{MgCl}_2$  solution (measured by a hydrometer in  $\text{kg/m}^3$ ) and  $\rho_{\text{H}_2\text{O}}$  is density of water. The specific gravity of the saturated  $\text{MgCl}_2$  solution used here is 1.30 at  $21^\circ\text{C}$ .



**Figure 3.1** Crushed salt.



**Figure 3.2** Sieve analysis apparatus.

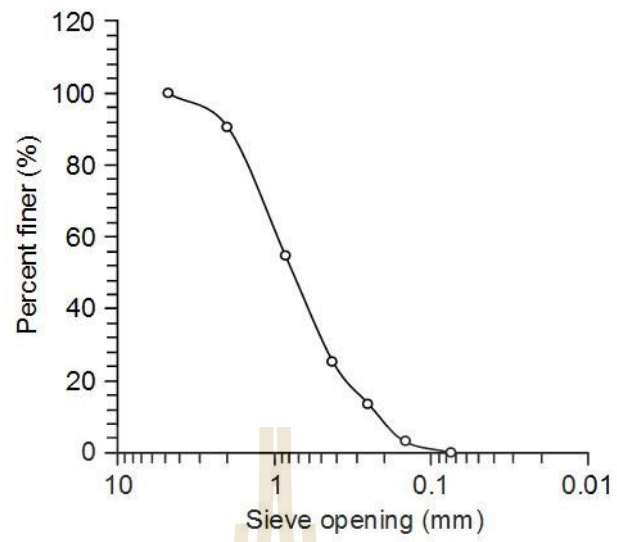


**Figure 3.3** Grain size distribution of crushed salt.



# CHAPTER IV

## LABORATORY TEST METHOD

### 4.1 Introduction

The objective of the laboratory testing is to determine the consolidation behavior and mechanical properties of crushed salt mixed with saturated  $\text{MgCl}_2$  solution as affected by the applied stresses and consolidation periods. This chapter describes the test apparatus and method.

### 4.2 Test apparatus

#### 4.2.1 Test cylinder

The consolidation test can be performed by installed crushed salt mixed with saturated  $\text{MgCl}_2$  solution in the cylindrical stainless-steel tube. The steel tube consists of tube with inner diameter is 54 mm, the outer diameter is 64 mm, and the height is 200 mm. Two load platens having 53 mm diameter with 100 mm length are used to applied axial constant axial stresses on the crushed salt specimens. A drained hole with diameter of 10 mm is in the center of load platens. Two o-rings are installed around each load platen to seal gap between load platen and inner tube wall (Figure 4.1).

#### 4.2.2 Consolidation load frame

A consolidation load frame is used to apply constant axial stress to the crushed salt (Figure 4.2). The cantilever beam with pre-calibrated dead weight can apply a truly constant axial stress to the specimen.

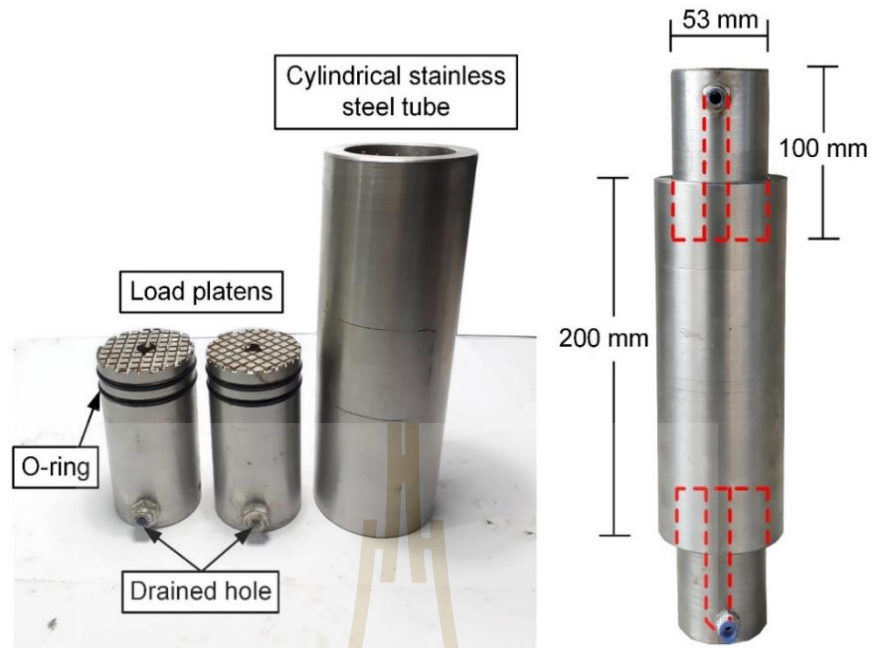


**Figure 4.1** Cylindrical stainless-steel tube for consolidation testing.

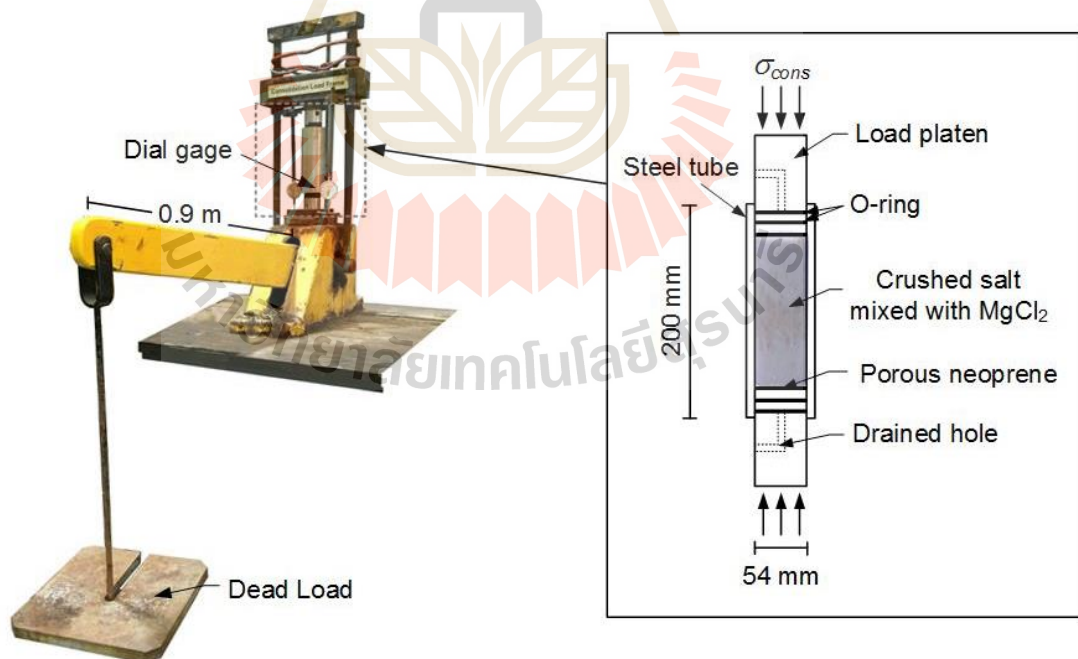


**Figure 4.2** Laboratory arrangement for consolidation testing.

### 4.3 Suitable saturated MgCl<sub>2</sub> solution content

The suitable saturated MgCl<sub>2</sub> solution content is determined by applying consolidation stresses ( $\sigma_{\text{cons}}$ ) from 2.5, 5.0, 7.5 to 10 MPa to the crushed salt mixed with saturated MgCl<sub>2</sub> solution from 0%, 5% to 10% by weight. All tests are conducted under ambient temperature. The crushed salt and saturated MgCl<sub>2</sub> solution are mixed thoroughly, poured into the steel tube, and lightly tapped to obtain a flat end. The initial length of specimen is obtained as 140 mm with initial volume of 320.63 cm<sup>3</sup> before inserting the loading. The initial densities before loading are 1.184, 1.300 and 1.340 g/cm<sup>3</sup> and initial porosity before loading are 45.15, 39.79% and 37.91% for the 0%, 5% and 10% saturated MgCl<sub>2</sub> solution contents. The results indicate that axial strain increases with saturated MgCl<sub>2</sub> solution content (Figure. 4.3). The dry crushed salt specimen shows the lowest consolidation. This agrees with the results obtained by Shor et al. (1981), Wang, et al. (1992) and Khamrat et al. (2016) that a small amount of fluid can significantly enhance the consolidation rate. The axial strains obtained at 5% and 10% saturated MgCl<sub>2</sub> solution contents are similar. The saturated solution content used in this study is therefore maintained constant at 5% by weight.

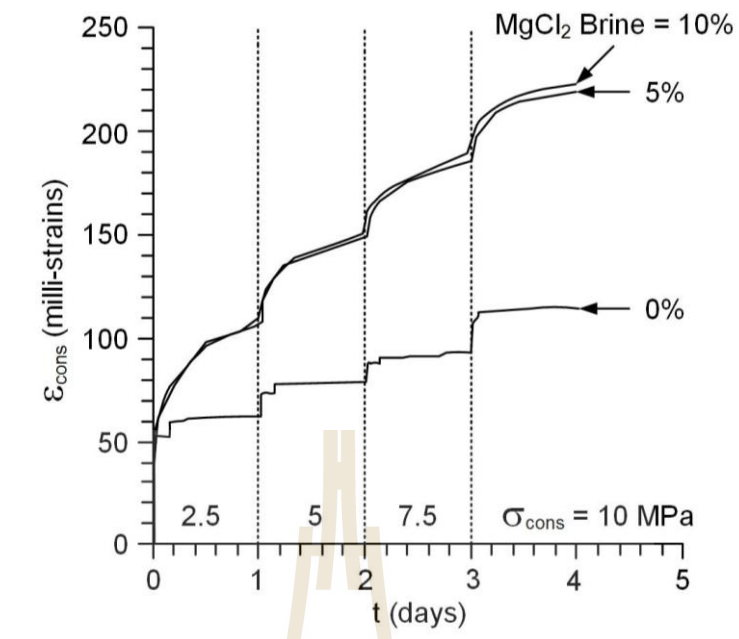


**Figure 4.3** Axial strains of consolidation crushed salt with saturated  $\text{MgCl}_2$  solution as a function of time for different axial stresses.



## 4.4 Test method

### 4.4.1 Consolidation test

The consolidation tests are performed by applying constant axial stresses on the crushed salt mixed with saturated  $\text{MgCl}_2$  solution installed in a cylindrical steel tube. A consolidation load frame applies constant stresses ranging from 2.5, 5, 7.5 to 10 MPa. All tests are conducted under ambient temperature for 7, 15, 30 and 90 days for each condition. The sample installation method is identical to that described in section 4.3. The axial deformation is monitored using displacement dial gages. They are used to calculate the axial strains of the specimen. The readings are made every one minute for the first hour. After that the reading intervals are gradually increased to every hour.

The consolidation magnitude (axial strains,  $\epsilon_{\text{cons}}$ ) can be calculated using the equation:

$$\epsilon_{\text{cons}} = \Delta L/L \quad (4.1)$$

where  $\epsilon_{\text{cons}}$  is axial strain of consolidated crushed salt mixture with saturated  $\text{MgCl}_2$  solution (mm/mm),  $\Delta L$  are length change overtime consolidated crushed salt (mm), and  $L$  is initial length of the installed specimens.

Density of the consolidated crushed salt ( $\rho_{\text{cons}}$ ) can be calculated using the equation:

$$\rho_{\text{cons}} = m/v \quad (4.2)$$

where  $\rho_{\text{cons}}$  is density of consolidated crushed salt ( $\text{g}/\text{cm}^3$ );  $m$  is weight of crushed salt specimens (g) and  $v$  is volume of specimens ( $\text{cm}^3$ ).

#### 4.5 Uniaxial compression tests method

The uniaxial compressive strength test procedure follows as much as practical the ASTM (D2938-95) standard practice and the ISRM suggested method. The compression tests are performed on the crushed salt specimens after removing from the steel tube for 7, 15, 30, and 90 days. The specimens are cut to obtain flat and parallel end surfaces. The length-to-diameter ratios ( $L/D$ ) are about 2.0-2.2 which comply with the specifications given by the ASTM standard practice (ASTM D4543-85). The axial stress is applied by a compression load frame (SBEL, Model PLT-75 POINT) (Figure. 4.4). The crushed salt samples are loaded at the constant rate of 0.5-1 MPa/second until failure. Neoprene sheets are used to minimize the friction at the interfaces between the loading platen and the sample surface. The axial and radial deformations are monitored using displacement dial gages with a precision of 0.001 mm. The elastic modulus ( $E$ ) and Poisson's ratio ( $\nu$ ) are determined from the tangent about 50% of the failure stress.

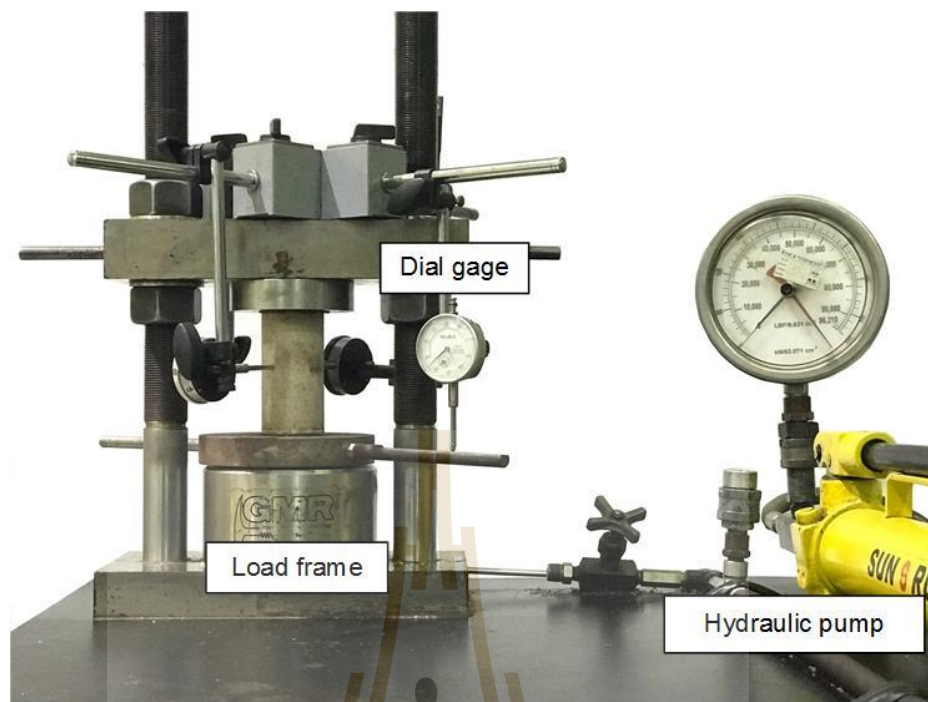


Figure 4.4 Arrangement for uniaxial compression teste.



# CHAPTER V

## LABORATORY TEST RESULTS

### 5.1 Introduction

This chapter describes the physical and mechanical property test results of consolidation crushed salt mixed with saturated  $\text{MgCl}_2$  solution as affected by the applied stress and consolidation period.

### 5.2 Consolidation test results

The consolidation test results under  $\sigma_{\text{cons}}$  of 2.5, 5, 7.5 and 10 MPa for 7, 15, 30 and 90 days indicate that higher applied consolidation stress ( $\sigma_{\text{cons}}$ ) leads to a larger strain and density (Table 5.1). The strains and density increase immediately after the axial stress is applied. The strain rates decrease with time, and tend to remain relatively constant after 30 days as shown in Figure 5.1. The density of specimen after removed from the steel tube are increases due to increasing the consolidation stress. The density increases rapidly within 3 days after consolidation. It approaches a constant value after 15 days.

The deformation of the crushed salt may be divided into two phases: instantaneous and transient deformations. The mechanism governing the instantaneous deformation is the rearrangement of the salt particles which occurs immediately after load application (Hwang et al., 1993; Callahan et al., 1996). The transient phase involves cracking and sliding between salt particles and creep deformation of the salt particles. This leads to the deceleration of the deformation.

**Table 5.1** Physical properties of crushed salt after consolidation.

$\sigma_{\text{cons}}$ (MPa)	Parameters	t (days)			
		7	15	30	90
2.5	$\rho_{\text{cons}}$ (g/cm <sup>3</sup> )	1.52	1.56	1.59	1.63
	$\epsilon_{\text{cons}}$ (milli-strains)	147.42	183.93	204.57	232.52
5	$\rho_{\text{cons}}$ (g/cm <sup>3</sup> )	1.58	1.61	1.63	1.66
	$\epsilon_{\text{cons}}$ (milli-strains)	161.89	193.39	223.29	260.34
7.5	$\rho_{\text{cons}}$ (g/cm <sup>3</sup> )	1.63	1.67	1.71	1.77
	$\epsilon_{\text{cons}}$ (milli-strains)	180.82	203.21	244.36	277.31
10	$\rho_{\text{cons}}$ (g/cm <sup>3</sup> )	1.69	1.76	1.80	1.86
	$\epsilon_{\text{cons}}$ (milli-strains)	201.86	216.54	265.61	300.52

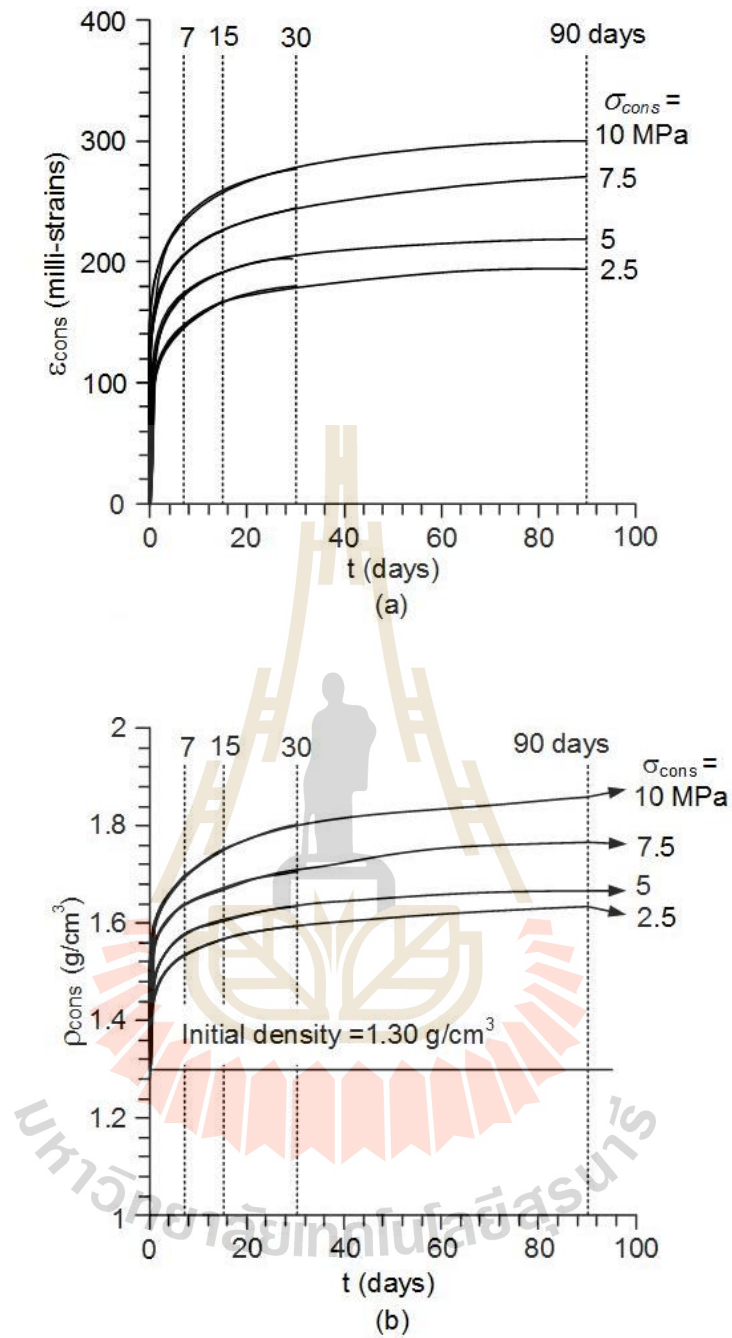


**Figure. 5.1** Axial strain (a) and Density (b) as a function of consolidation period ( $t$ ) for different consolidation stresses ( $\sigma_{cons}$ ).

### 5.3 Uniaxial compression test result

Figure 5.2 shows the stress-strain curves obtained from different consolidation stresses and periods. Larger consolidation period and stress lead to higher density, strength and elasticity of consolidated crushed salt specimens. Two main factors that influencing the physical and mechanical properties of the consolidated crushed salt specimen are mechanical and healing processes. The healing process is defined as a time-dependent consolidation process seem to be a main factor that governing the compressive strength of consolidated crushed salt specimens than do by the stresses (Table 5.2). The Poisson's ratios however decrease slightly with increasing consolidation period as shown in Table 5.2 and Figure 5.3. The results suggest that the crushed salt becomes denser, stiffer, stronger and less compressible with time and applied stress. The results obtained here reasonably agree with those of Khamrat et al. (2016) who perform the consolidation test on the same sources of crushed salt but mixed with NaCl brine. The specimens before and after uniaxial compressive strength testing are shown in Figure 5.4.

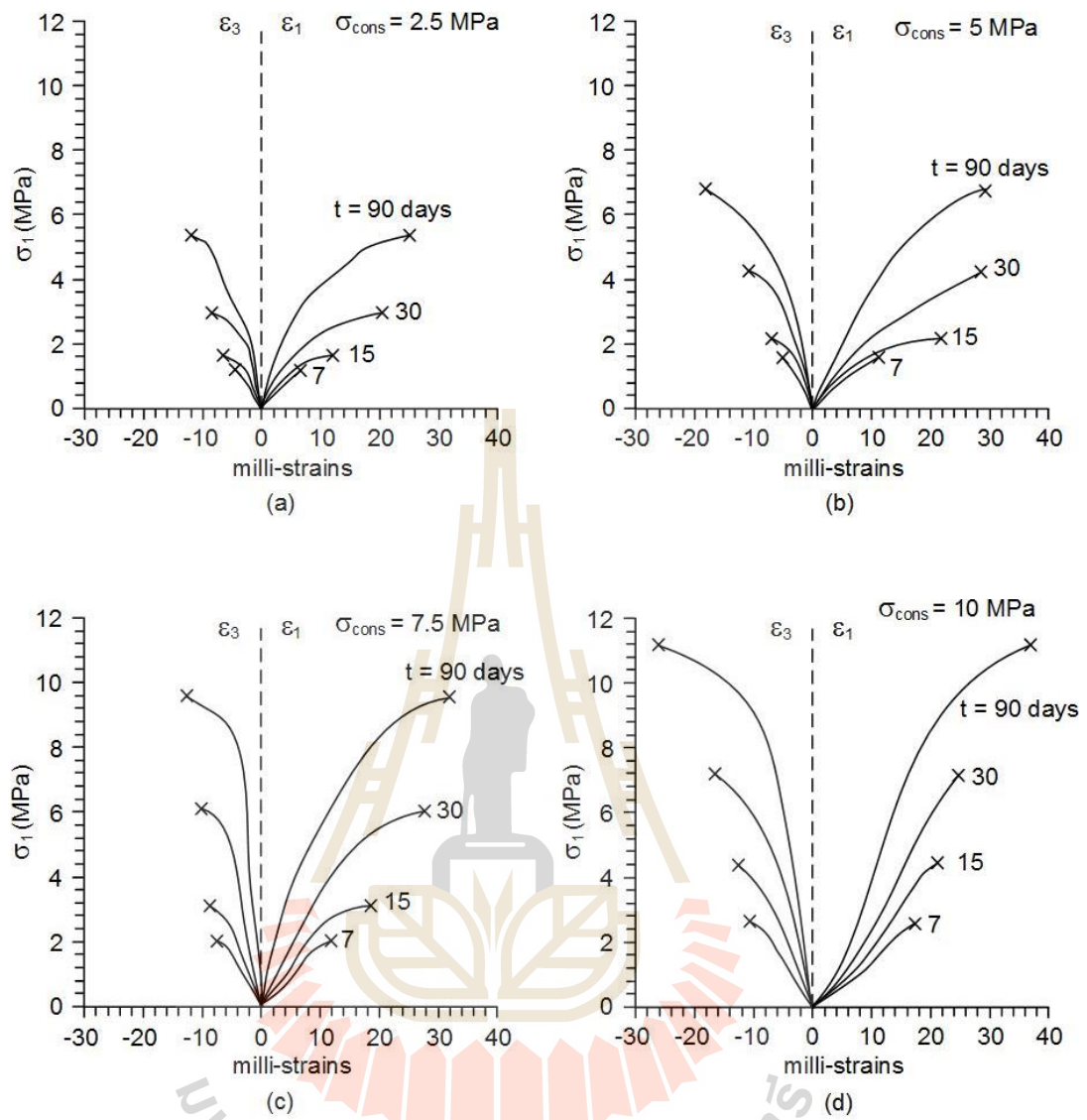


**Figure 5.2** Stress–strain curves obtained from uniaxial compression test of crushed salt specimens after consolidation.

**Table 5.2** Mechanical properties of crushed salt after consolidation.

$\sigma_{\text{cons}}$ (MPa)	Parameters	t (days)			
		7	15	30	90
2.5	$\rho$ (g/cm <sup>3</sup> )	1.52	1.54	1.58	1.62
	$\sigma_c$ (MPa)	1.12	1.62	2.97	5.32
	E (MPa)	150	192	224	269
	$\nu$	0.36	0.35	0.34	0.33
5	$\rho$ (g/cm <sup>3</sup> )	1.56	1.61	1.63	1.67
	$\sigma_c$ (MPa)	1.62	2.34	4.22	6.72
	E (MPa)	179	213	261	303
	$\nu$	0.35	0.34	0.33	0.32
7.5	$\rho$ (g/cm <sup>3</sup> )	1.64	1.68	1.70	1.76
	$\sigma_c$ (MPa)	2.03	3.12	5.94	9.51
	E (MPa)	210	247	290	330
	$\nu$	0.34	0.33	0.32	0.31
10	$\rho$ (g/cm <sup>3</sup> )	1.68	1.75	1.78	1.86
	$\sigma_c$ (MPa)	2.66	4.37	7.03	11.67
	E (MPa)	246	271	314	377
	$\nu$	0.33	0.32	0.31	0.30

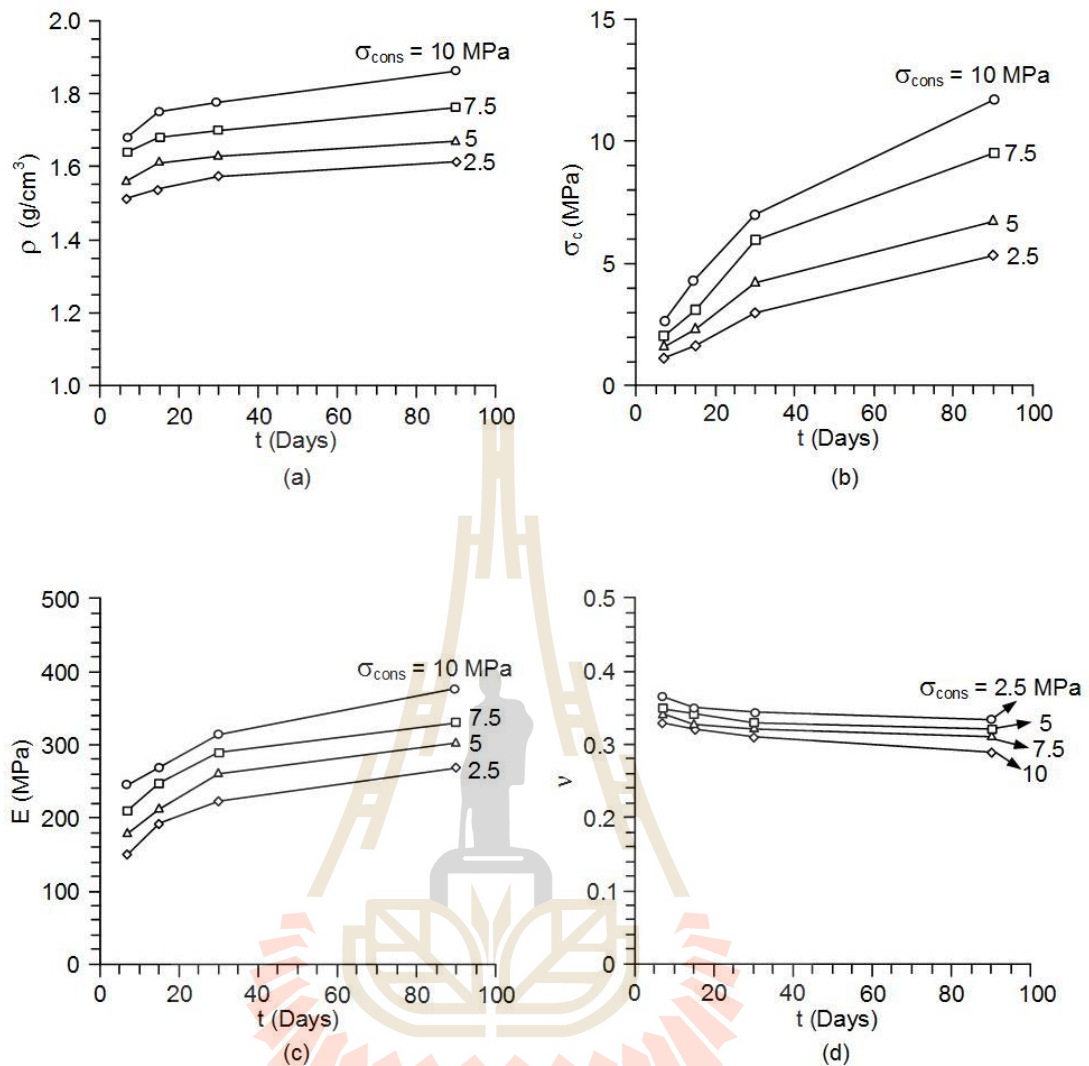


**Figure 5.3** Density (a), Poisson's ratio (b), Uniaxial compressive strength (c) and elastic modulus (d) as a function of consolidation period ( $t$ ) for different consolidation stresses ( $\sigma_{\text{cons}}$ ) of consolidation crush salt mixed with saturated  $\text{MgCl}_2$  solution.

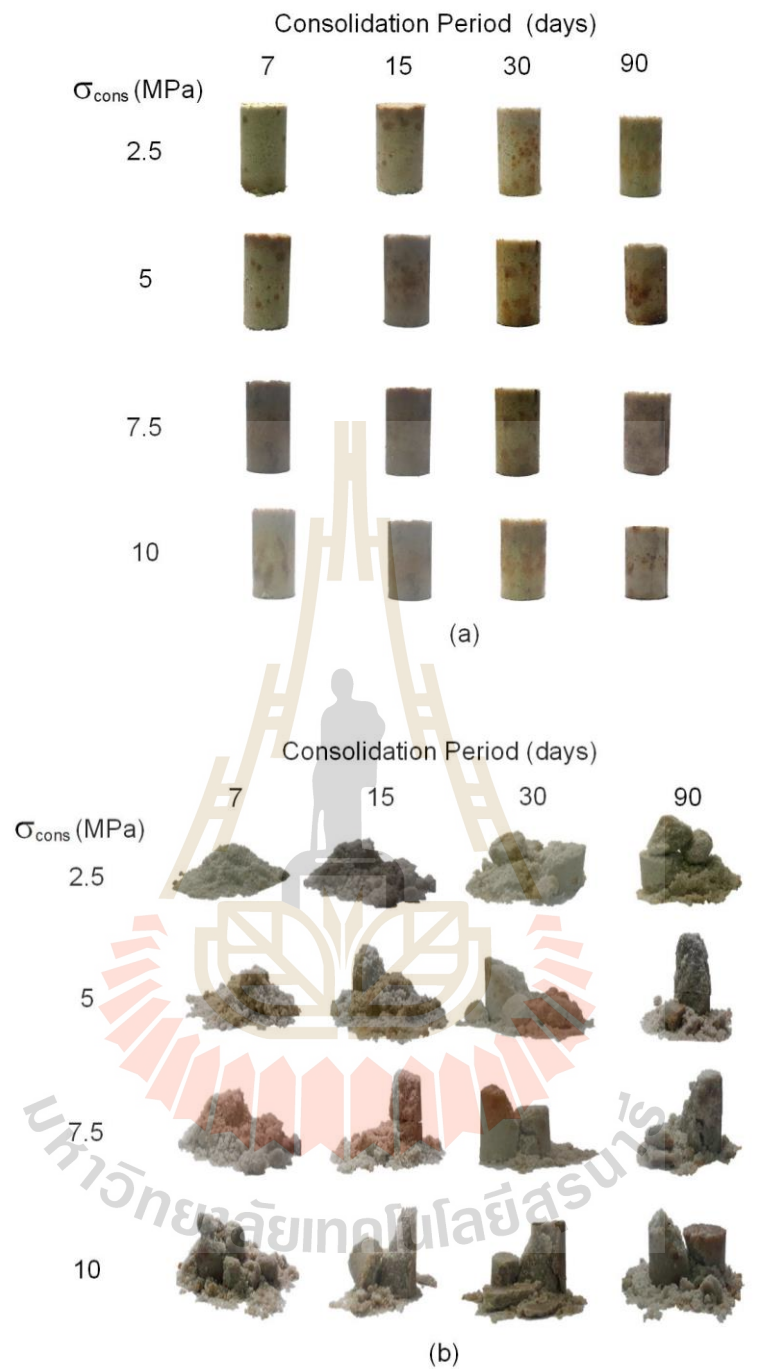


**Figure 5.4** Consolidated specimens before (a) and after (b) uniaxial compression test.

## CHAPTER VI

### DEVELOPMENT OF EMPIRICAL EQUATIONS

#### 6.1 Introduction

This chapter describe the application of strain energy density principle to describe the consolidated crushed salt mixed with saturated MgCl<sub>2</sub> solution under different stresses and periods. The crushed salt properties (density, porosity, uniaxial compressive strength and elastic modulus) are used to develop a set of empirical equations as a function of mean strain energy and consolidation period. The regression analysis on the test data using IBM SPSS Statistics software (Wendai, 2000) is

#### 6.2 Strain energy density principle

The mean strain energy density required to consolidate the crushed salt mixed with saturated MgCl<sub>2</sub> solution under different stresses and periods is calculated from the test results. It is postulated that the crushed salt can be consolidated by applying the mean strain energy ( $W_m$ ) which can be calculated from the applied mean stresses ( $\sigma_m$ ) and strains ( $\epsilon_m$ ) (Jaeger et al., 2007):

$$W_m = \frac{3}{2}(\sigma_m \cdot \epsilon_m) \quad (6.1)$$

$$\sigma_m = \frac{1}{3}(\sigma_1 + \sigma_2 + \sigma_3) \quad (6.2)$$

$$\varepsilon_m = \frac{1}{3} (\varepsilon_1 + \varepsilon_2 + \varepsilon_3) \quad (6.3)$$

For the consolidation test performed here, the lateral stresses  $\sigma_2$  and  $\sigma_3$  on the specimen are equal and can be calculated as a function of time based on the uniaxial strain condition, i.e. assuming that no lateral strain of the specimen occurs in the thick-wall steel tube during consolidation. The axial strains from the measurement results, therefore, represent the volumetric strain:

$$\sigma_2 = \sigma_3 = \left[ \frac{\nu}{(1 - \nu)} \right] \sigma_1 \quad (6.4)$$

where  $\nu$  is Poisson's ratio, and  $\sigma_1$  is consolidation stress ( $\sigma_{\text{cons}}$ ). Table 6.1 gives the calculated mean stress, strain and strain energy density for different consolidation stresses and durations. The specimens under higher consolidation stress and time are obtained under higher mean strain energy densities.

### 6.3 Reconsolidated crushed salt properties as a function of mean strain energy density

The physical and mechanical properties of crushed salt mixed with saturated  $\text{MgCl}_2$  solution can be correlated with the applied mean strain energy density during consolidation. It is first postulated that two main mechanisms govern the changes of the properties of crushed salt: consolidation and healing. The first mechanism involves the volumetric reduction of the crushed salt mass by particle rearrangement, creep, cracking and sliding between grain boundaries. It is reflected by instantaneous and transient deformations which are mainly controlled by the applied energy. The

second mechanism involves the healing between salt particles (Hwang et al., 1993; Hansen, 1997). This mechanism does not decrease the crushed salt volume. It can however strengthen and stiffen the specimen as the consolidation period increases.

**Table 6.1** Mean stresses and strains and mean strain energy densities applied to crushed salt during consolidation periods.

$\sigma_{\text{cons}}$ (MPa)	Parameters	Consolidation period (days)			
		7	15	30	90
2.5	$\sigma_m$ (MPa)	1.79	1.74	1.71	1.67
	$\varepsilon_m$ ( $10^{-3}$ )	49.1	54.0	60.3	67.3
	$W_m$ (kPa)	132	141	154	168
5	$\sigma_m$ (MPa)	3.45	3.33	3.31	3.23
	$\varepsilon_m$ ( $10^{-3}$ )	61.3	64.5	67.7	72.2
	$W_m$ (kPa)	318	329	336	350
7.5	$\sigma_m$ (MPa)	5.09	4.91	4.87	4.74
	$\varepsilon_m$ ( $10^{-3}$ )	68.2	74.4	81.5	88.5
	$W_m$ (kPa)	520	459	595	630
10	$\sigma_m$ (MPa)	6.61	6.47	6.33	6.05
	$\varepsilon_m$ ( $10^{-3}$ )	72.2	86.8	92.4	100.2
	$W_m$ (kPa)	769	842	877	910

Based on the concept above the change of the crushed salt density ( $\rho$ ) can be represented by:

$$\rho = \rho_{\text{initial}} + \Delta\rho_{\text{cons}} \quad (6.5)$$

where  $\rho_{\text{initial}}$  is the initial density before applying the mean strain energy (equal to 1.30 g/cm<sup>3</sup>) and  $\Delta\rho_{\text{cons}}$  is the reduction of bulk density due to the strain energy and consolidation period. Regression analysis of the test data by SPSS software (Colin and Paul 2012) can determine  $\Delta\rho_{\text{cons}}$  as a function of  $W_m$  and  $t$ :

$$\Delta\rho_{\text{cons}} = 0.348W_m^{0.346}t^{0.107} \quad (\text{g/cm}^3) \quad (6.6)$$

Good correlation is obtained ( $R^2 > 0.9$ ). Figure. 6.1 compares the curve fits with the test results. It should be noted that the crushed salt density is independent of the healing mechanism because this mechanism does not reduce the bulk volume of specimens.

Similar to the density prediction above, the reduction of crushed salt porosity ( $n$ ) during consolidation can be determined by the regression analysis of the test data:

$$n = n_{\text{initial}} - \Delta n_{\text{cons}} \quad (6.7)$$

where  $n_{\text{initial}}$  is the initial crushed salt porosity (39.79%) and  $\Delta n_{\text{cons}}$  is the porosity reduction which can be represented by a power equation:

$$\Delta n_{\text{cons}} = 16.38W_m^{0.346}t^{0.107} \quad (\%) \quad (6.8)$$

The diagrams in Figure. 6.2 suggest that the applied mean strain energy affects the porosity reduction and the density increase more than does the consolidation period.

The crushed salt strength ( $\sigma_c$ ) is controlled by consolidation energy and period, which can be determined from the test data as:

$$\sigma_c = 1.29W_m^{0.560}t^{0.490} \quad (\text{MPa}) \quad (6.9)$$

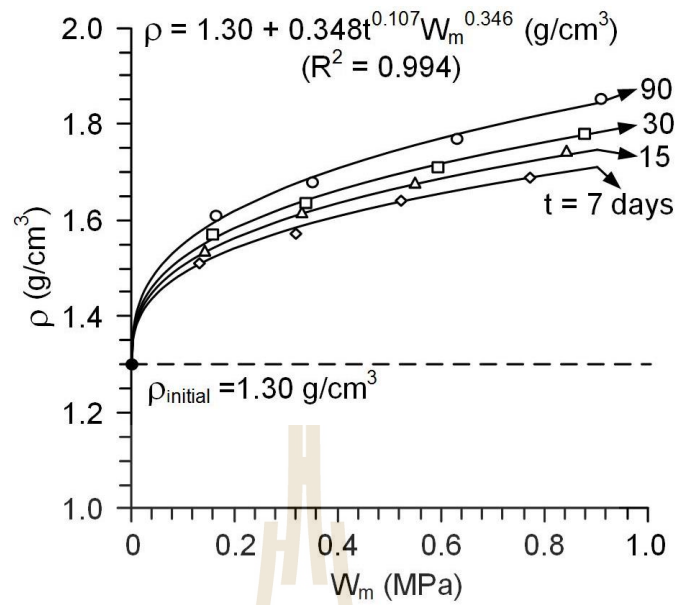
The crushed salt strength increases with the the consolidation period. Figure 6.3 compares the predictions with the test results.

The crushed salt elastic modulus (E) is also controlled by both consolidation energy and period:

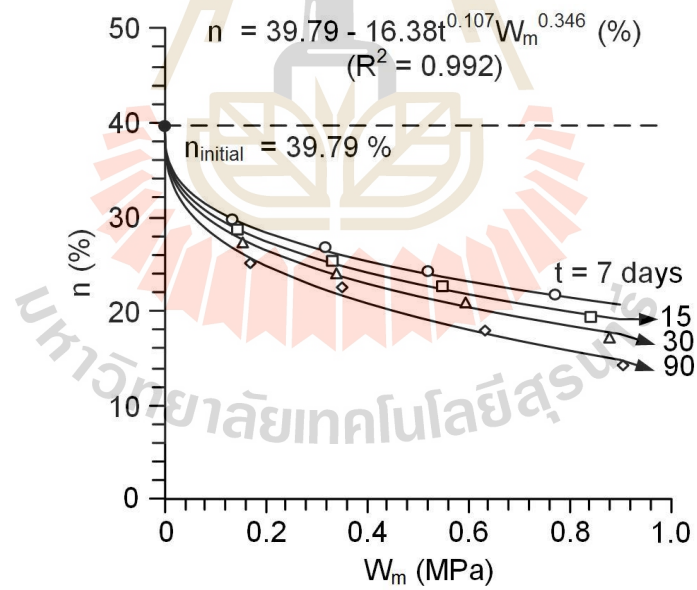
$$E = 176W_m^{0.220}t^{0.175} \quad (\text{MPa}) \quad (6.10)$$

Figure 6.4 shows that the elasticity of crushed salt can increase with time.

The relationships between the mechanical properties of the crushed salt and its mean strain energy required during each consolidation period as shown in Figures 6.1 through 6.4 can be used to predict the performance of crushed salt backfill under in-situ condition as described in the following chapter.



**Figure 6.1** Density ( $\rho$ ) as a function of mean strain energy density.



**Figure 6.2** Porosity ( $n$ ) as a function of mean strain energy density.

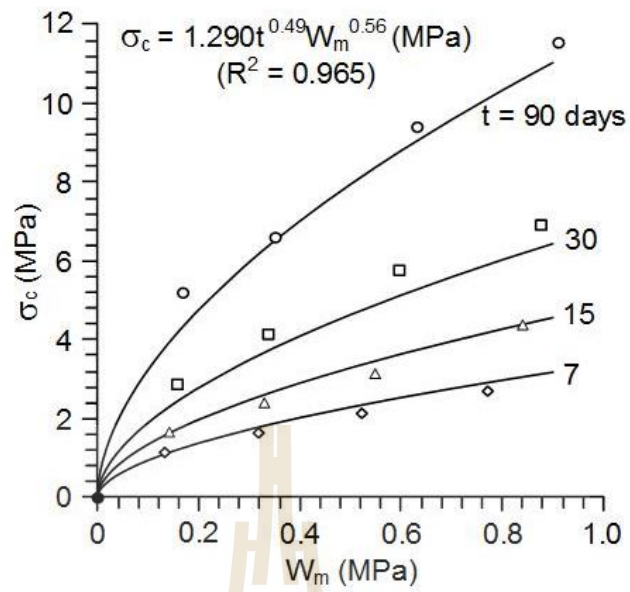


**Figure 6.3** Uniaxial compressive strength ( $\sigma_c$ ) as a function of mean strain energy density.

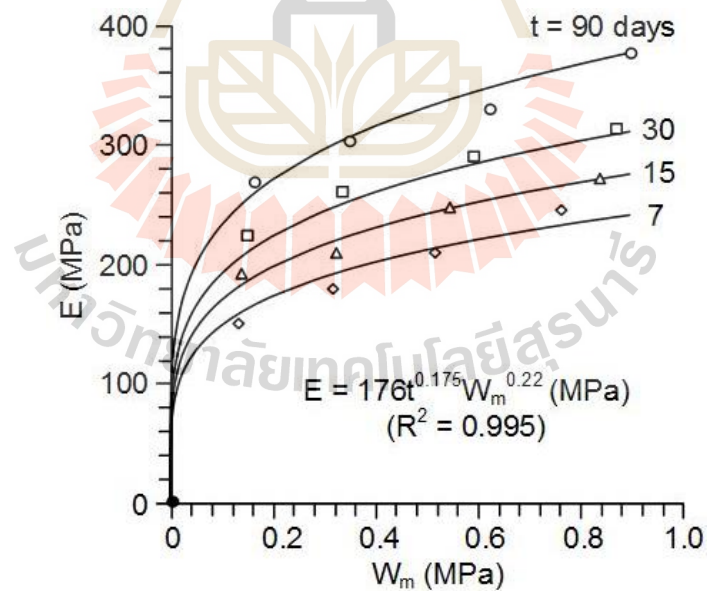


**Figure 6.4** Elastic modulus ( $E$ ) as a function of mean strain energy density.

# CHAPTER VII

## CRUSHED SALT BACKFILL PROPERTIES

### 7.1 Introduction

This chapter describe predictions of the crushed salt backfill properties after emplaced in long-wall circular opening. The time-dependent closure of long-wall circular opening is calculated in terms of the released mean strain energy density. The crushed salt properties are predicted for different carnallite contents (C%), external pressures (P<sub>o</sub>) and installation periods.

### 7.2 Long-wall circular opening in salt mass subjected to uniform external pressure

The mean strain energy released by creep closure of long-wall circular opening in infinite domain subjected to uniform external pressure (in-situ stress) is determined and used to predict the changes of the crushed salt properties after emplacement. The released energy (W<sub>m,s</sub>) can be calculated from the stresses and strains at the opening boundary as:

$$W_{m,s} = \frac{3}{2} \left[ \left\{ \frac{1}{3} (\sigma_r + \sigma_\theta + \sigma_z) \right\} \cdot \left\{ \frac{1}{3} (\varepsilon_r + \varepsilon_\theta + \varepsilon_z) \right\} \right] \quad (7.1)$$

where  $\sigma_r$ ,  $\sigma_\theta$  and  $\sigma_z$  are radial, tangential and axial stresses and  $\varepsilon_r$ ,  $\varepsilon_\theta$  and  $\varepsilon_z$  are radial, tangential and axial strains.

Under plane strain condition the radial, tangential and axial stresses from obtained the Kirsch's solution can be presented as (Jaeger et al. 2007):

$$\sigma_r = \left[ 1 - \left( \frac{a^2}{r^2} \right) \right] \cdot P_o \quad (7.2)$$

$$\sigma_\theta = \left[ 1 + \left( \frac{a^2}{r^2} \right) \right] \cdot P_o \quad (7.3)$$

$$\sigma_z = \nu(\sigma_r + \sigma_\theta) \quad (7.4)$$

where  $P_o$  is external pressure,  $a$  is opening radius and  $r$  is radial distance from the center.

For a long-wall circular opening in time-dependent medium, such as carnallite and salt, the induced strains can be determined as:

$$\varepsilon_r = \varepsilon_r^e + \varepsilon_r^c \quad (7.5)$$

$$\varepsilon_z = \varepsilon_\theta = 0 \quad (7.6)$$

where  $\varepsilon_r^e$  is the elastic radial strain and  $\varepsilon_r^c$  is the time-dependent radial strain controlling the creep closure of the opening.

The elastic radial strain can be obtained by (Jaeger et al. 2007):

$$\varepsilon_r^e = \frac{1}{E} [(1 - \nu^2)\sigma_r - \nu(1 + \nu)\sigma_\theta] \quad (7.7)$$

Nair and Boresi (1970) and Fuenkajorn and Daemen (1988) have derived the radial creep strain around circular hole based on the potential creep law and the associated flow rule as:

$$\varepsilon_r^c = \frac{3}{2} \kappa (\sigma^*)^{(\beta-1)} \cdot S_r (t_1^\gamma - t_0^\gamma) \quad (7.8)$$

where  $\kappa$ ,  $\beta$  and  $\gamma$  are material constants of the potential creep law,  $S_r$  is the radial stress deviation,  $\sigma^*$  is the equivalent (effective) stress,  $t_0$  is time at which loading is applied (usually assumed to be zero) and  $t_1$  is time at which the strains are calculated. The stress deviation can be obtained from:

$$S_r = \sigma_r - \frac{1}{3} (\sigma_r + \sigma_\theta + \sigma_z) \quad (7.9)$$

Based on the von Mises flow rule,  $\sigma^*$  is defined as:

$$\sigma^* = \frac{1}{\sqrt{2}} \{ (\sigma_r - \sigma_\theta)^2 + (\sigma_\theta - \sigma_z)^2 + (\sigma_z - \sigma_r)^2 \}^{\frac{1}{2}} \quad (7.10)$$

Substituting equations (7.2) to (7.10) into Eq. (7.1) the released mean strain energy (by closure) at the boundary of long-wall circular opening can be calculated.

To determine the released of the mean strain energy from the long-wall circular opening in salt and carnallite from the equations above, the mechanical and rheological properties of the materials are required. Wilalak and Fuenkajorn (2016) and Luangthip et al. (2016) have calibrated these properties from the rock salt specimens with various carnallite contents. To demonstrate the application of the strain energy concept used here,

the calibrated parameters from these investigators are applied. Table 7.1 gives the mechanical and rheological parameters for rock salts with different carnallite contents,  $C\% = 0, 20, 40$  and  $60\%$  by weight. The released energy at the opening boundary is calculated for the external pressures of 5.5 and 8 MPa (equivalent to the depths approximately of 200 and 300 m). Figure 7.1 plots the released strain energy density ( $W_{m,s}$ ) as a function of time after excavation. The  $W_{m,s}$  increases rapidly particularly during the first year. The rate of releasing energy reduces with time. The greater external pressures (deeper opening) lead to the larger released energy. Higher carnallite contents ( $C\%$ ) yield higher released mean strain energy. This is primarily governed by large radial creep strains due to the low values of  $E$  and  $K$  of the higher carnallite content materials.

**Table 7.1** Mechanical and rheological properties of Maha Sarakham salt and carnallite (Wilalak and Fuenkajorn 2016; Luangthip et al. 2016).

carnallite contents ( $C\%$ )	$\kappa \cdot 10^3$ ( $\text{MPa}^{-1} \cdot \text{day}^{-1}$ )	$\beta$	$\gamma$	$E$ (GPa)	$\nu$
Pure halite	0.44	1.4	0.19	16.81	0.26
20	0.7	1.43	0.2	11.04	0.3
40	1.1	1.46	0.21	7.26	0.34
60	1.75	1.49	0.23	4.77	0.38

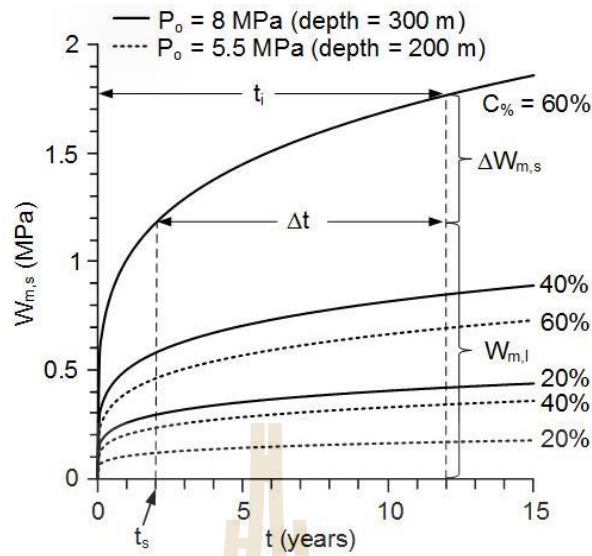


**Figure 7.1** Mean strain energy density ( $W_m$ ) released from closure of long-wall circular opening in potash with different carnallite contents ( $C\%$ ) for depths of 200 m and 300 m.

### 7.3 Prediction of crushed salt properties after emplacement

To predict the crushed salt properties after emplacement, the strain energy left for the consolidation is needed. It can be obtained from:

$$\Delta W_{m,s} = W_{m,s} - W_{m,l} \quad (7.11)$$

where  $W_{m,s}$  is the total released energy after drilling to any selected period ( $t_i$ ) determined as if no seal is installed, and  $W_{m,l}$  is the energy lost due to creep closure before backfill installation. For this demonstration, the  $\Delta W_{m,s}$  at depths of 200 and 300 m are calculated for  $t_s = 2$  years. The prediction period ( $\Delta t$ ) is up to 10 years after excavation. The time at which the backfill is installed is designated as  $t_s$  in Figure. 7.1. Salt mass with higher

carnallite content and greater depth can release greater mean strain energy than that of the lower ones. The duration for consolidation ( $\Delta t$ ) can be obtained from:

$$\Delta t = t_i - t_s \quad (7.12)$$

From equation (7.11) the remaining strain energy,  $\Delta W_{m,s}$ , can be calculated as a function of  $\Delta t$  as shown in Figure. 7.2. The results indicate that the  $\Delta W_{m,s}$  values increase with time ( $\Delta t$ ). This is due to the fact that the released energy by creep closure of the opening after backfill emplacement is contributed by the increase of the radial stresses and the decrease of the radial strain rate at the opening boundary. This is caused by the mechanical interaction between the opening wall and the installed crushed salt. The diagram in Figure. 7.2 suggest that the time at which the backfill is installed is more critical for deep openings than for the shallow ones.

Substituting  $\Delta W_{m,s}$  and  $\Delta t$  from Figure. 7.2 into  $W_m$  and  $t$  values in equations (6.5) through (6.10) the density, porosity, compressive strength and elastic modulus can therefore be predicted. For this demonstration the predictions are made up to 10 years. The results suggest that the crushed salt density increases with time ( $\Delta t$ ) from its initial value of  $1.30 \text{ g/cm}^3$  (Figure. 7.3). Subsequently the corresponding porosity decreases with  $\Delta t$  (Figure. 7.4). Without applying  $W_m$ , the density and porosity of the crushed salt seal remain unchanged. Both  $\sigma_c$  and  $E$  increase with  $P_o$  and  $\Delta t$  (Figure. 7.5, 7.6). Under no  $W_m$  application  $\sigma_c$  and  $E$  will not increase. The results indicate that the properties of crushed salt backfill can improve significantly more for opening in high  $C\%$  rock salt than those in lower  $C\%$  rock salt. This is primarily because  $C\%$  makes the surrounding rock salt soften and results in a larger creep rate.

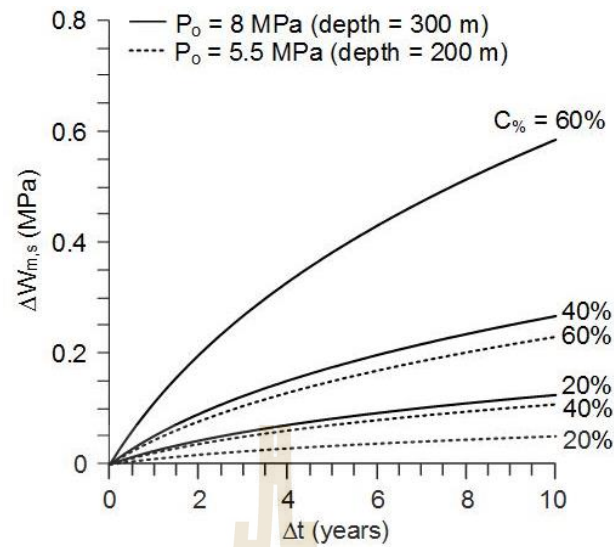


**Figure.7.2** Remaining mean strain energy density ( $\Delta W_m$ ) as a function of time after backfill emplacement (at year 2) under different carnallite contents ( $C\%$ ).

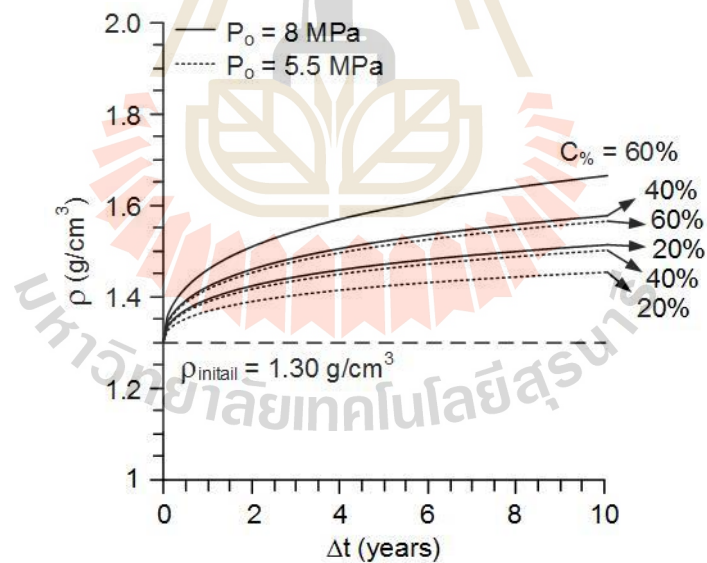


**Figure 7.3** Density ( $\rho$ ) of crushed salt backfill as a function of time after emplacement in long-wall circular opening for different carnallite contents ( $C\%$ ).

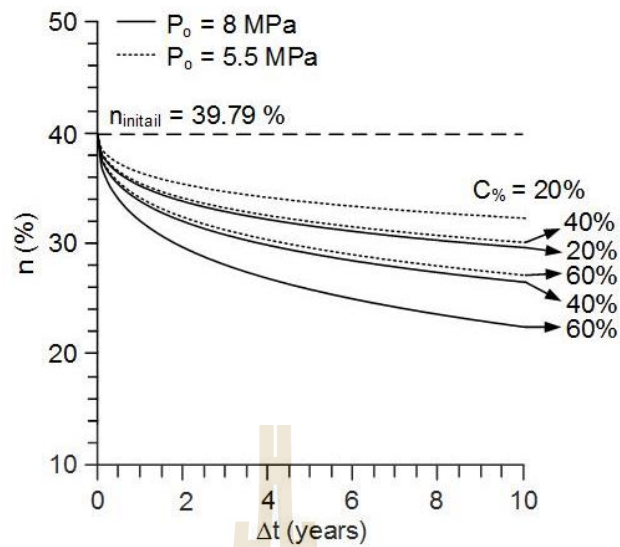


**Figure 7.4** Porosity ( $n$ ) of crushed salt backfill as a function of time after emplacement in long-wall circular opening for different carnallite contents ( $C\%$ ).

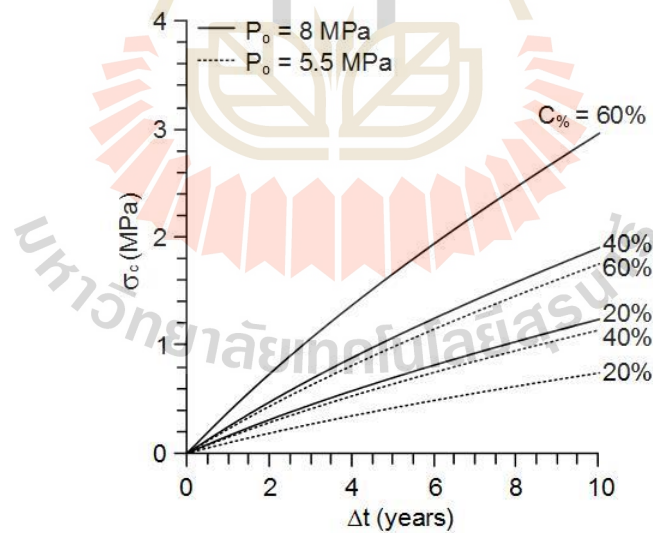


**Figure 7.5** Uniaxial compressive strength ( $\sigma_c$ ) of crushed salt backfill as a function of time after emplacement in long-wall circular opening for different carnallite contents ( $C\%$ ).

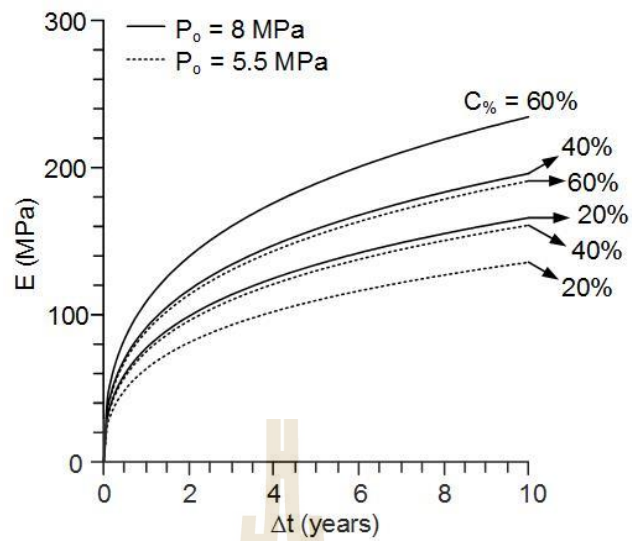


**Figure 7.6** Elastic modulus ( $E$ ) of crushed salt backfill as a function of time after emplacement in long-wall circular opening for different carnallite contents ( $C\%$ ).

## CHAPTER VIII

### DISCUSSIONS AND CONCLUSIONS

#### 8.1 Discussions

The chapter discusses the physical and mechanical properties of consolidation crushed salt mixed with saturated  $MgCl_2$  solution for use as backfill material in potash mines, and comparisons of the results from this study with those obtained elsewhere under similar test conditions.

A total of crushed salt mixed with saturated  $MgCl_2$  solution have been consolidated under periods of 7 to 90 days. The results are reliable as evidenced by the overlapping (repeating) of the measured axial strains under different periods with the same  $\sigma_{cons}$ . The consolidation have been performed on a range of different consolidation periods (7, 15, 30 and 90 day) and consolidation stresses (2.5, 5, 7.5 and 10 MPa). The specimens are obtained from Lower member of Maha Sarakham formation. The initial densities before loading are  $1.30 \text{ g/cm}^3$  and initial porosity before loading are 39.79%. The results in Figure 5.1 show that the axial strain and density increase with the applied consolidation stresses and periods. The axial strain rates decrease with consolidation periods, and tend to remain relatively unchanged after 30 days.

The density, strength, elastic parameters and poisson's ratio of the crushed salt after being consolidated are determined under various stresses and durations. The results in Table 5.2 show that the density, strength and elasticity increase with consolidation period and stress. The Poisson's ratio decreases with time and stress. The results lead

to the development of the empirical formulae relating the crushed salt properties with the applied mean strain energy density.

The application of the strain energy principle allows considering both stress and strain to which the crushed salt specimens are subjected (Figures. 6.1 through 6.4). This approach is considered more fundamental and simpler than those of the complex creep and healing constitutive equations proposed elsewhere for the sealing of nuclear waste repository.

The prediction of the crushed salt properties after emplacement in exploratory opening of excavation presented here may be conservative because the axial load imposed by the seal gravity is excluded from the calculation. Depending on the emplacement depth the weight of the crushed salt seal can contribute to the mean strain energy applied to the crushed salt.

The diagrams in Figures 7.3 through 7.6 can be used as a guideline for the backfill planning and for the performance assessment of the crushed salt backfill properties. Care should be taken to apply the results obtained here to other salt formations and locations. Different grain size distributions and moisture contents of the crushed salt are likely to result in different consolidation behaviors.

The method proposed here to predict the physical and mechanical properties of consolidated crushed salt mixed with saturated  $MgCl_2$  solution after installation may be applicable to the experimental results obtained by other researchers (e.g., Wang et al. 1992; IT Corporation 1987; Case et al. 1987).

The mathematical relationships between the crushed salt properties, consolidation period and mean strain energy density are needed for the predictions. It should be noted that the properties of the consolidated crushed salt after installation

will improve only if it is installed in the openings excavated in time-dependent rocks; such as salt and potash, where there is creep closure of the opening after excavation.

The mechanical properties predictions are also sensitive to the creep parameters of the surrounding rock. Application of different constitutive creep models for the surrounding salt mass may also result in different predictions of the crushed salt properties.

The mechanical properties of crushed salt mixed with saturated  $\text{MgCl}_2$  solution are different from the crushed salt mixed with  $\text{NaCl}$  solution, as performed by Khamrat et al. 2016, because crushed salt mixed with saturated  $\text{MgCl}_2$  solution does not have recrystallization process. A comparison between the properties of crushed salt mixed with saturated  $\text{MgCl}_2$  solution and with  $\text{NaCl}$  solution is summarized in Table 8.1 showing that the density and Poisson's ratio of crushed salt mixed with saturated  $\text{MgCl}_2$  solution are higher than those of  $\text{NaCl}$  solution. The uniaxial compressive strength and elastic modulus of the saturated  $\text{MgCl}_2$  solution mixtures are lower than those of the  $\text{NaCl}$  solution mixture.

**Table 8.1** Mechanical properties of crushed salt after consolidation under  $\sigma_{\text{cons}} = 10$  MPa for 90 days comparing between crushed salt mixed with  $\text{NaCl}$  and Saturated  $\text{MgCl}_2$  solution (Khamrat et al. 2016).

Saturated Solution	Parameters			
	$\rho$ ( $\text{g/cm}^3$ )	$\sigma_c$ (MPa)	E (MPa)	$\nu$ (%)
NaCl	1.58	15.07	439	0.29
Saturated $\text{MgCl}_2$ solution	1.86	7.65	377	0.30

Figure 8.1 compares the backfills performance between the two mixtures. The density and elastic modulus of crushed salt mixed with saturated  $MgCl_2$  solution are higher than those of the crushed salt mixed with  $NaCl$  solution. The uniaxial compressive strength and porosity of crushed salt mixed with saturated  $MgCl_2$  solution are lower than crushed salt mixed with  $NaCl$  solution.



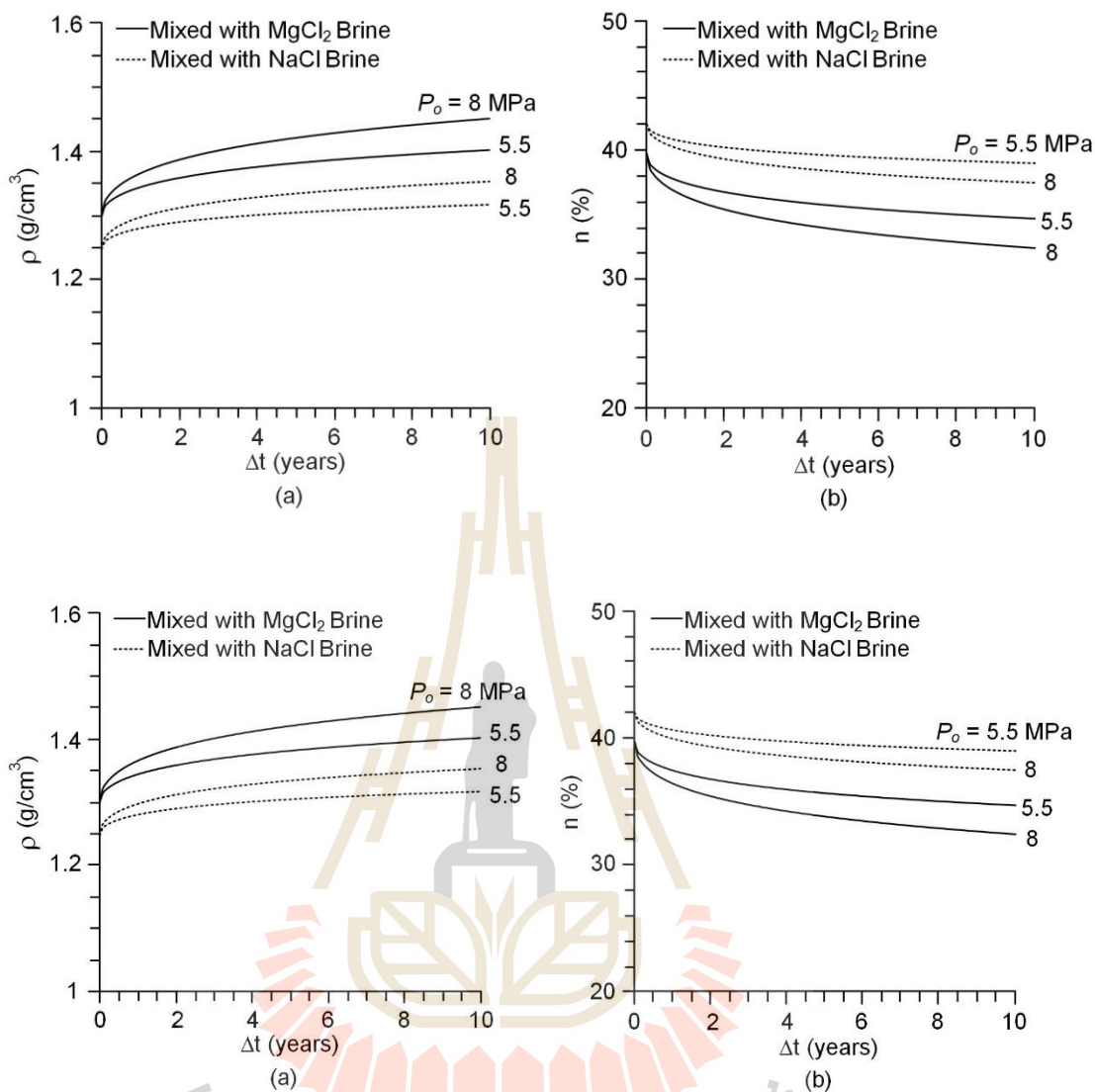


**Figure 8.1** Density (a), porosity (b), uniaxial compressive strength (c) and elastic modulus (d) of crushed salt backfill mixed with saturated MgCl<sub>2</sub> solution and NaCl solutions as a function of time after emplacement in rock salt (Khamrat et al. 2016).

## 8.2 Conclusions

All objectives and requirements of this study have been met. The results of the laboratory testing and analyses can be concluded as follows:

1) The crushed salt obtains for consolidation test have been grain size ranging from 0.075 to 4.75 mm. The specific gravity of the saturated  $\text{MgCl}_2$  solution used here is 1.30 at  $21^\circ\text{C}$

2) The consolidation of crushed salt mixed with saturated  $\text{MgCl}_2$  solution increases with increasing saturated  $\text{MgCl}_2$  solution content. The optimum solution content for the crushed salt is 5% by weight. The results of consolidation test show that the axial strain and density increase with increasing consolidation stress and period, which agrees with Ran and Daemen (1995) and Somtong et al. (2015).

3) Uniaxial compressive strength and elastic modulus of the crushed salt specimens increase with the consolidation stress and period. The consolidation stresses of 2.5 MPa for consolidation period of 7 days shows the lowest compressive strength, (about 1.12 MPa) and elastic modulus (150 MPa). The highest compressive strength is observed under 10 MPa consolidation stresses, which is about 11.67 MPa. The elastic modulus is 377 MPa after 90 days of consolidation.

4) The initial density and porosity are equal to  $1.30 \text{ g/cm}^3$  and 39.79%. The relationships between compressive strength, elastic modulus density and Poisson' ratio as a function of consolidation stress and consolidation period can be represented by a power equation.

5) The development of the empirical formulae of crushed salt properties implies that there are two main mechanisms occurring during consolidation: consolidation and healing. The first mechanism involves the volumetric reduction by

particle rearrangement, cracking and creep of salt crystals. It is reflected by instantaneous and transient deformations which are mainly controlled by the applied energy. The second mechanism involves the healing process between salt particles (Hwang et al. 1993; Hansen 1997). Both can strengthen and stiffen the crushed salt specimens.

6) The crushed salt properties after emplacement show that the greater external pressures (deeper opening) lead to the larger released energy. Higher carnallite contents (C%) of the surrounding salt yield higher released mean strain energy.

7) The crushed salt density increases with time ( $\Delta t$ ) while the initial value of  $1.30 \text{ g/cm}^3$ . Subsequently the corresponding porosity decreases with  $\Delta t$  while the initial value of 39.79%. Without applying  $W_m$ , the density and porosity of the crushed salt seal remain unchanged. The uniaxial compressive strength ( $\sigma_c$ ) and elastic modulus (E) increase with external pressure ( $P_o$ ) and  $\Delta t$ . Under no  $W_m$  application  $\sigma_c$  and E will not increase.

### **8.3 Recommendations for future studies**

The test results for consolidation of crushed salt mixed with saturated  $\text{MgCl}_2$  solution have been limited to consolidation stresses and time. To confirm the conclusions drawn in this study, more testing is required as follows:

1. More testing is required on a variety of carnallite - crushed salt mixtures with different percents of salt : carnallite ratios.
2. Consolidation test should be performed on a wider range of consolidation periods and consolidation stresses.

3. Effect of grain size distributions for the consolidation test should be determined.

4. Investigations of the relationship between elevated temperature and mechanical properties of consolidation crushed salt mixed with saturated  $\text{MgCl}_2$  solution may be desirable for deep mines.



## REFERENCES

- ASTM D4543-85. Standard practice for preparing rock core specimens and determining dimensional and shape tolerances. **Annual Book of ASTM Standards**, American Society for Testing and Materials, West Conshohocken, P.A.
- ASTM D2938-95. Standard test method for unconfined compressive strength of intact rock core specimens. **Annual Book of ASTM Standards**, American Society for Testing and Materials, West Conshohocken, PA.
- Brodsky, N.S. and Munson, D.E. (1991). The effect of brine on the creep of WIPP salt in laboratory tests. In **Proceedings of the Thirty - second U.S. Symposium on Rock Mechanics**. Norman, Oklahoma.
- Brodsky, S., Zeuch, H., and Holcomb, J. (1995). Consolidation and permeability of crushed WIPP salt in hydrostatic and triaxial compression. In **Proceedings of the Thirty - fifth US Symposium on Rock Mechanics** (pp. 497-502).
- Case, J.B. and Kelsall, P. (1987). Laboratory investigation of crushed salt consolidation. **International Journal of Rock Mechanics and Mining Sciences and Geomechanics Abstracts**. 25(5): 216-223.
- Case, J.B., Kelsall, P.C., and Withiam, J.L. (1987). Laboratory investigation of crushed salt consolidation. In **Proceedings of the Twenty - eighth U.S. Symposium on Rock Mechanics (USRMS)**. Tucson, Arizona.
- Callahan, G.D., Loken, M.C., Hurtads, L.D., and Hansen, F.D. (1996). Evaluation of constitutive models for crushed salt. In **Proceedings of the Fifth Mechanical**

- Mechanical Behavior of Salt** (pp 317-330). Clausthal-Zellerfeld, Germany.
- Callahan, G.D. and Hansen, F.D. (2002). Crushed salt constitutive model. In **Proceedings of the Basic and Applied Salt Mechanics** (pp. 239-252).
- Down, G.R.B. and McMullen, J. N (1985). The effect of inter particulate friction and moisture on the crushing strength of sodium chloride compacts. **Powder Technology**. 42(2): 169-174.
- Fossum, A.F., Callahan, G.D., Van Sambeek, L.L., and Senseny, P.E. (1988). How should one-dimensional laboratory equations be cast into three-dimensional. In **Proceedings of the Twenty-ninth U.S. Symposium on Rock Mechanics** (pp. 35-41). Minneapolis, Rotterdam.
- Fuenkajorn, K. and Daemen, J.J.K. (1988). Borehole closure in salt. **PhD. Thesis, University of Arizona, U.S.A.**
- Fu, X., Huck, D., Makein, L., Armstrong, B., Willen, U., and Freeman, T. (2012). Effect of particle shape and size on flow properties of lactose powders. **Particuology**. 10(2): 203-208.
- Guises, R., Xiang, J., Latham, J.P., and Munjiza, A. (2009). Granular packing: numerical simulation and the characterization of the effect of particle shape. **Granular Matter**. 11(5): 281-292.
- Holcomb, D.J. and Hannum, D.W. (1982). **Consolidation of Crushed-Salt Backfill under Conditions Appropriate to the WIPP facility**. Rep. No. SAND82-0630, Sandia National Laboratories, Albuquerque, NM.
- Hein, H.J. (1991). **Ein Stoffgesetz zur Beschreibung des thermo-mechanischen Verhaltens von Steinsalzgranulat**. Thesis Technical University Aachen.

- Hwang, C.L., Wang, M.L., and Miao, S. (1993). Proposed healing and consolidation mechanisms of rock salt revealed by ESEM. **Microscopy Research and Technique**. 25(5-6): 456-464.
- Hansen, F.D. (1997). Reconsolidating salt: compaction, constitutive modeling, and physical processes. **International Journal of Rock Mechanics and Mining Sciences**. 34(3-4): 119.e1–119.e12.
- Hansen, F.D. and Mellegard, K.D. (2002). Mechanical and permeability properties of dynamically compacted crushed salt. In **Proceedings of the Basic and Applied Salt Mechanics** (pp. 253-256).
- IT Corporation (1987). **Laboratory Investigation of Crushed Salt Consolidation and Fracture Healing**. Rep. No. BMI/ONWI-631, Columbus, OH.
- Jaeger, J.C., Cook, N.G.W., and Zimmerman, R.W. (2007). **Fundamentals of Rock Mechanics**. 4th ed. Blackwell, Australia.
- Kelsall, P.C., Case, J.B., Nelson, J.W., and Franzone, J.G. (1984). **Assessment of Crushed Salt Consolidation and Fracture Healing in a Nuclear Waste Repository in Ralt**. D'Appolonia Waste Mangement Services.
- Khamrat, S., Tepnarong, P., Artkhonghan, K., and Fuenkajorn, K. (2016). Crushed salt consolidation for borehole sealing in potash mines. **International Journal of Geotechnical and Geological Engineering**. 36(1): 49–62.
- Loken, M.C. and Statham, W. (1997). Calculation of density and permeability of compacted crushed salt within an engineered shaft sealing system. **Computing in Civil Engineering**. pp. 485-492.

- Lee, R. and Souza, E.D. (1998). The effect of brine on the creep behavior and dissolution chemistry of evaporites. **Canadian Geotechnical Journal**. 35: 720-729.
- Luangthip, A., Khamrat, S., and Fuenkajorn, K. (2016). Effects of carnallite contents on stability and extraction ratio of potash mine. In **Proceedings of the 9th Asian Rock Mechanics Symposium**. Bali, Indonesia.
- Miao, S., Wang, M.L., and Schreyer, H.L. (1995). Constitutive models for healing of materials with application to compaction of crushed rock salt. **Journal of Engineering Mechanics**. 121(10): 1122-1129.
- Nair, K. and Boresi, A.P. (1970). Stress analysis for time dependent problems in rock mechanics. In **Proceedings of the 2nd Congress of the International Society for Rock Mechanics** (pp. 531-536). Belgrade.
- Olivella, S. and Gens, A. (2002). A constitutive model for crushed salt. **International Journal for Numerical and Analytical Methods in Geomechanics**. 26: 719-746.
- Pfeifle, T.W., Senseny, P.E., and Mellegard, K.D. (1987). **Influence of Variables on the Consolidation and Unconfined Compressive Strength of Crushed Salt**. Technical Report BMI/ONWI-627, Prepared by RE/SPEC, Inc., Rapid city, SD.
- Pfeifle, T.W. (1991). **Consolidation, permeability, and strength of crushed salt/bentonite mixtures with application to the WIPP**. Rep. No. SAND90-7009, Sandia National Laboratories, Albuquerque, NM.
- Pudewills, A. and Krauss, M. (1999). Implementation of a viscoplastic model for crushed salt in the ADINA program. **Computers and Structures**. 72(1-3): 293-299.

- Ran, C. and Daemen, J.J.K. (1995). The influence of crushed salt particle gradation on compaction. In **Proceedings of The Thirty-fifth U.S. Symposium on Rock Mechanics** (pp.761-766). Reno, NV, A.A. Balkema, Rotterdam.
- Shor, A.J., Baes, C.F., and Canonico, C.M. (1981). **Consolidation and Permeability of Salt in Brine**. Rep. No. ORNL-5774, Oak Ridge National Laboratory, Oak Ridge, TN.
- Salzer, K., Popp, T., and Böhnelt, H. (2007). Mechanical and permeability properties of highly pre-compacted granular salt bricks. In **Proceedings of the sixth Conference on the Mechanical Behavior of Salt** (pp.239-248). Hannover, Germany.
- Somtong, S., Khamrat, S., and Fuenkajorn, K. (2015). Laboratory performance assessment of consolidated crushed salt for backfill material in potash mine openings. **Research and Development Journal of the Engineering Institute of Thailand**. 26(1): 15-22.
- Theerapun, C., Khamrat, S., Sartkeaw, S., and Fuenkajorn, K. (2017). effects of backfill compositions on the integrity of underground salt and potash mines. **Engineering Journal of Research and Development**. 28(2).
- Van Sambeek, L.L. (1992). Testing and modelling of backfill used in salt and potash mines. In **Proceedings of the Rock Support in Mining and Underground Construction** (pp. 583-589). Balkema, Rotterdam.
- Wang, M.L., Miao, S.K., Maji, A.K., and Hwang, C.L. (1992). Effect of water on the consolidation of crushed rock salt. In **Proceedings of the Engineering Mechanics** (pp. 531-534). ASCE.

Wang, M.L., Maji, A.K., and Miao, S. (1994). **Deformation mechanisms of WIPP backfill. Technical Completion Report.** U.S. Department of Energy.

Wendai, L. (2000). **Regression Analysis, Linear Regression and Profit Regression, In 13 Chapters; SPSS for Windows: Statistical Analysis.** Publishing House of Electronics Industry, Beijing.

Wilalak, N. and Fuenkajorn, K. (2016). Constitutive equation for creep closure of shaft and borehole in potash layers with varying carnallite contents. In **Proceedings of the Ninth Asian Rock Mechanics Symposium.** Bali, Indonesia



## **BIOGRAPHY**

Mr. Worwat Suwannbut was born on August 15, 1994 in Nakhon Ratchasima Province, Thailand. He received his Bachelor's Degree in Engineering (Geological Engineering) from Suranaree University of Technology in 2017. For his post-graduate, he continued to study with a Master's degree in the Geological Engineering Program, Institute of Engineering, Suranaree university of Technology. During graduation, 2017-2019, he was a part time worker in position of research assistant at the Geomechanics Research Unit, Institute of Engineering, Suranaree University of Technology. He published technical paper related to rock mechanics, titled consolidation of crushed salt mixed with saturated  $MgCl_2$  brine in the Proceeding of the 12th South East Asia Technical University Consortium (SEATUC) Symposium 2018, University Gadjah Mada, Yogyakarta, Indonesia.

มหาวิทยาลัยเทคโนโลยีสุรนารี